UiT
NORGES
ARKTISKE
UNIVERSITET

Faculty of Science and Technology
Department of Geosciences

Rapid temperature rise may have triggered glacier surges all over Svalbard

Erik Schytt Holmlund

Master thesis in Geology (GEO-3900), June 2020

This thesis is dedicated to John Walter Gregory (1864–1932), as his theories of global warming-related surging were largely forgotten, but are today more relevant than ever.

Abstract

Observational and geomorphological records suggest that most glaciers on Svalbard reached their maximum Little Ice Age extents by means of surging. Furthermore, it seems to have happened within just a few decades, suggesting that the rapid concurrent changes in climate might have triggered this widespread surging. The specific precipitation and temperature range of Svalbard seems optimal for glacier surges, and areas with a climatic trend toward the same range may therefore exhibit more glacier surging in the future. This is important, as surges contribute significantly to overall melt and sea-level rise when they occur, and the potential for it to spread is essential to study further. To understand the phenomenon better, five glaciers in Bolterdalen and Foxdalen on Svalbard were studied in depth. Observational, geomorphological, photogrammetric, and ground penetrating radar data indicate that four out of five glaciers seemed to have surged between 1896 and 1936. On average, they lost 81% ± 7% of their volumes between 1936 and 2019, twice as much as the one glacier that did not show signs of surging. In addition, the glacier Scott Turnerbreen lost 90.4% ± 5.4 of its volume in the same interval, in a previously undescribed kind of surge where it did not terminate in stagnation directly, but instead continued to advance for many years. This *surge and post-surge advance* phase occurred over between 22 and 47 years, making it the longest dynamically driven advance ever recorded on Svalbard. The results indicate that climate change-triggered surging may expedite subsequent melt by multiple times, highlighting the immense need to study the phenomenon further and include it in future ice-loss projections.

Acknowledgements

A complete list of people that have contributed to this thesis would be longer than the thesis itself. I would primarily like to thank my supervisor, Lena Håkansson, for financial, academic and moral support since this project started in the autumn of 2017. Thank you Andy Hodson for help with snowmobile logistics and financing, and for unofficial supervision during the longer part of this project. In addition, I want to thank my father Per Holmlund and my fiancée Anna Bøgh for many constructive additions to the project and thesis. Thank you Kris Barrett, Sindre Kolbjørnsgaard and Petter Schytt Winberg for a joint collaboration in the 2019 Glacier Rephotography Project, in which the recaptured historic photographs were taken. This project would not have reached its current state if not for the countless discussions with researchers and primarily students, at UNIS and in conferences over the years. Thank you Heïdi Sevestre in particular, for the many invaluable discussions around your work, which has shaped this project to what it is today.

People that have helped in the field include, but are not limited to; Amélie Roche, Ursula Enzenhofer, Jóhanna Jóhannesdóttir, Rakul Johannesen, Emiliano Santin, Arne Kreiensiek, Anna Bang Kvorning, Ampere (Eirik Hellerud's dog), Guillaume Mercier, Anna Sartell, Philipp Schmid, Marjolein Gevers, Mark Furze and Elias Lundström. Indeed, the majority of students and leading experts that have contributed to this project are women, and I therefore regret the fact that 82% of the main authors that I have cited are male. I do not feel that this is representative of today's research environment, but literature is thankfully shifting, and the number of cited men are "only" twice as many since 2000. Finally, I want to thank the staff at UNIS and UiT for enabling this opportunity, especially Kai Mortensen at UiT for invaluable student advising.

Contents

List of Figures

List of Tables

1

Introduction

The archipelago of Svalbard is majorly covered by ice, but this cover is decreasing at an alarming rate. After a general glacier expansion during the Little Ice Age (LIA), ice cover has decreased by around 13% to a total cover of 57% today, and this rate of decrease has approximately tripled in the last ~30 years (Martín-Moreno et al., 2017; Nuth et al., 2013). The exact time of the turning point from growth to decline is still unclear, as measured positions of glaciers since the late 1800s do not always give the same retreat signal. Most glaciers in northern Fennoscandia showed a synchronous response to early 1900s warming by starting to retreat in the 1910s (Ahlmann, 1953; Karlén, 1973; Holmlund and Holmlund, 2019). On Svalbard, however, estimations or mentions of the *LIA-termination* range from before the 1900s (Liestøl, 1988; Lefauconnier and Hagen, 1991; Svendsen and Mangerud, 1997), near the 1900s (e.g. Hansen, 2003; Hambrey, 2005; Mangerud and Landvik, 2007) or up to the 1920s or 1930s (Dowdeswell et al., 1995; Farnsworth et al., 2016, 2017; Humlum et al., 2005). This timing inconsistency between studies is understandable as numerous amounts of glacier surges occurred in the same timeframe (Hagen et al., 1993; Lefauconnier and Hagen, 1991; Liestøl, 1969; Schytt, 1969). The high frequency of glacier surges amid general retreat was indeed brought up as it happened, but it has yet to be truly understood (Gregory et al., 1897; Nathorst, 1900). Surging enables a glacier to advance due to dynamic instabilities instead of linearly responding to changes in temperature and precipitation, and connecting glacier fluctuations to climate change is therefore more difficult where this phenomenon is common (Meier and Post, 1969). The drivers of glacier surges are however important to understand, as many recent surges

have been major contributors to mass loss and sea-level rise (Dunse et al., 2015; Nuth et al., 2019; Willis et al., 2018).

The glaciers of Svalbard surge more frequently than anywhere else in the world, which complicates the distinction between climatically and dynamically driven advances (Figure 1.1; Sevestre and Benn, 2015). However, the number of observed surges seems to have decreased during the 1900s, compared to the drastically higher apparent frequency near the end of the LIA (Dowdeswell et al., 1995; Ottesen et al., 2017; Nuth et al., 2019; Sevestre et al., 2015). To emphasise, the earliest observed surge on Svalbard is from 1839 (Recherchebreen; Liestøl, 1969), and all observations were made after this year. Therefore, they do not represent the LIA as a whole, but rather the *end of it*. Coupled with the recent findings that many or most glaciers seemed to have reached their maximum late-LIA extents by means of surging (Figure 1.2; Farnsworth et al., 2016), there is a dire need to further understand what happened. Rapid temperature variations occurring synchronously with many glacier surges have confused the story of Svalbard's glaciers for over a century, but with the recent findings that climate may control surging, an explanation may be that these phenomena are interconnected.

Nordenskiöld Land is the least glaciated region on Svalbard, and it houses the main settlements of Longyearbyen and Barentsburg. The climate around Longyearbyen is warmer and drier than most other areas on Svalbard, making it less optimal for larger glaciers to form (Figures 1.2, 1.3). Most glaciers in the region are today cold-based, but many show strong signs of having had a much more dynamic warm-based past (Bælum and Benn, 2011; Hodgkins et al., 1999; Sevestre et al., 2015). The first known observations of the region's glaciers were by the Conway Expedition in 1896 who tried to cross Spitsbergen for the first time (Conway, 1897; Garwood and Gregory, 1898; Gregory et al., 1897). They classified many terrestrial glaciers as "Arctic glaciers", which were flatter, ended in cliffs, and "their rate of flow may be much more rapid than that of Alpine glaciers" (Conway, 1897; Garwood and Gregory, 1898). One glacier was studied in more detail (Booming Glacier, today Drønbreen; 78.12°*N* 16.8°*E*), and they questioned whether its aggressive front and its upper part's "sunken appearance", were due to either a cooling or a warming of the climate, and argued for the latter (Gregory et al., 1897). This glacier was most likely surging, proven by their descriptions and photographs, probably along with all of the other glaciers that they said were similar. Some of these depicted areas have later been studied in more detail, including the valley Bolterdalen just east of Longyearbyen. It houses the glacier Rieperbreen, whose post-surge forefield geomorphology has been of interest (Lyså and Lønne, 2001), and Scott Turnerbreen, whose 1900s history gave testament to the immense effect a surge can have on the subsequent melt rates and dynamics of a glacier (Hodgkins et al., 1999). The neighbours Ayerbreen, Foxbreen and Fleinisen have not been

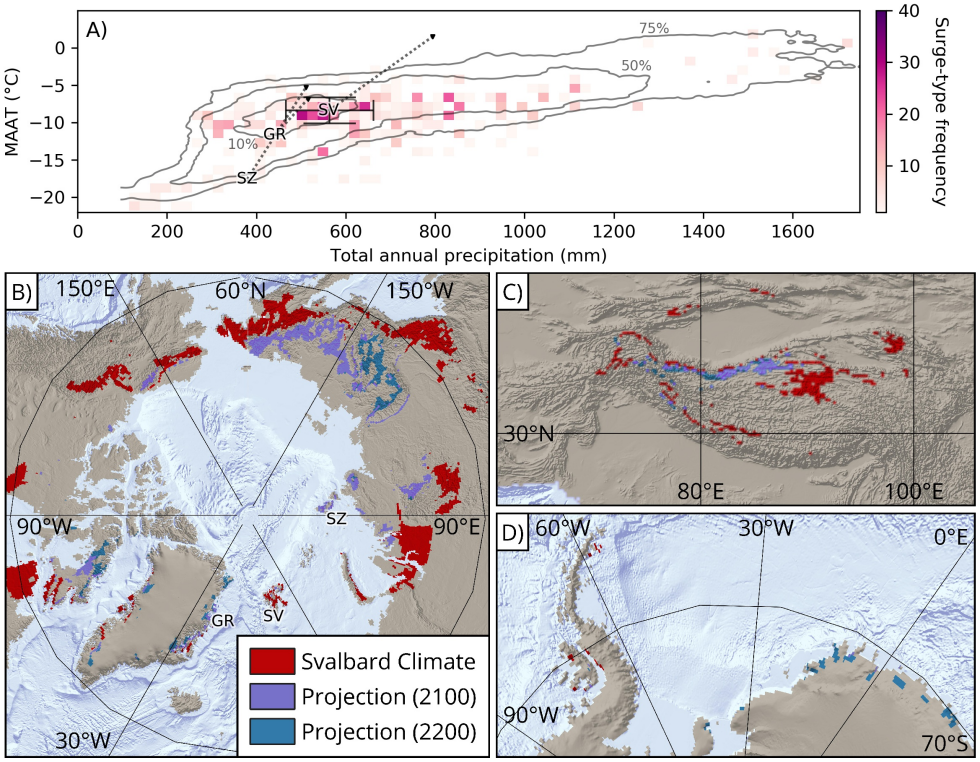

Figure 1.1: A) The climate of Svalbard (SV) coincides with the highest frequency of recorded glacier surges. The standard deviation of the archipelago's climate (error bars) is used to define a *Svalbard climate* range. Linear climate projections for 2100 (shown as triangles), assuming the same trend as in 1979–2019, for north-eastern Greenland (GN; 76°N, 21°W) and Servernaya Zemlya (SZ; 80°N, 96°E) show that their trajectory (dotted line) intersects the current climate of Svalbard. Contour lines outline where most of the world's glaciers reside (total = 177281). The densest area is outlined by the 10% line, and the density gradually decreases outward. **B)** Arctic areas that are currently within the *Svalbard climate* range, according to ERA5 data in 1979–2019, and areas that are projected to reach it before 2100 and 2200, assuming a constant linear trend. **C)** and **D)** show the same projection for the Himalayas and the west Antarctic, respectively.

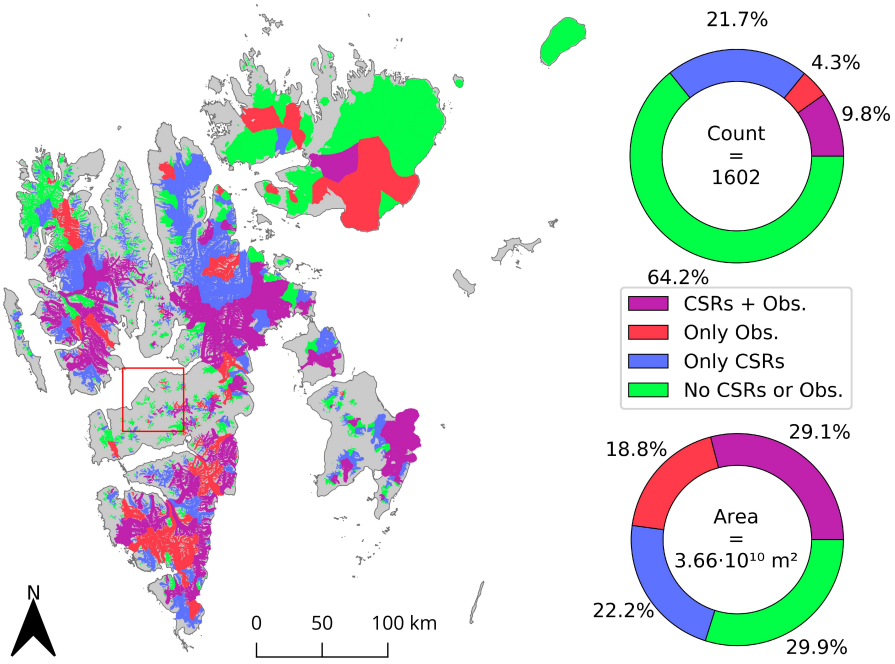

Figure 1.2: Distribution of observed surges on Svalbard and the presence of CSRs in glacier forefields. Observation and CSR data are from Farnsworth et al. (2016) and glacier outlines are from Nuth et al. (2013). The surrounding of Longyearbyen (central Nordenskiöld Land) is outlined in red (Figure 1.3).

given the same attention, but they have an equally rich story to tell. The history of Bolterdalen and the neighbouring Foxdalen is therefore interesting to study in detail, as surging seems to have been a frequent phenomenon in the past, and could shed further light on why and when glaciers on Svalbard surged (Figure 1.4).

The aim of this study is to shed light on the connection between Svalbard's rapid changes in climate, and the high concurrent frequency of glacier surges close to the LIA termination. This is put in a global perspective by updating the work of Sevestre and Benn (2015), to identify the current climatic setting of glaciers that have surged, and also which areas have a climatic trend toward the same setting. The glaciers in the Bolterdalen and Foxdalen valleys on Svalbard have been studied in depth, as they provide good examples of the many glaciers that seemed to have surged within just a few decades of each other. The implications of connecting widespread glacier surging to rapid climate change are huge, as other regions might gain order-of-magnitude larger melt rates in the future. Further work is needed to conclusively prove this interconnection, but it is vital to consider, as we may need to account for this in projections about the future of all glaciers.

1.1 Setting

The geologic history of Svalbard affects both where glaciers can be found and how they act with the surrounding landscape. The eastern and western coasts of Svalbard generally consist of Precambrian crystalline rocks (Norwegian Polar Institute, 2016). Due to the immense tectonic activity between the Paleocene and Early-Eocene, the centre of Spitsbergen houses basins of younger sedimentary deposits, which are much easier to erode and enable a higher sediment supply for the antecedent glaciers (Steel et al., 1981). On a millennial time-scale, glacial activity had the most influential effect on the landscape. During the Last Glacial Maximum (LGM), approximately 21 000 years ago (21 ka), the whole archipelago was covered in ice, except possibly a few mountain peaks (Hughes et al., 2016; Westergaard et al., 2011). The post-LGM deglaciation was rapid, and most shelves and fjords were deglaciated by the Lateglacial–Holocene transition at 11.7 ka (Hormes et al., 2013). However, many subsequent sporadic readvances occurred all over Svalbard from around 12–9 ka, and the only current explanation is by surging due to the rapid climatically induced geometric changes that occurred (Farnsworth et al., 2018). Between this period and the LIA, faint signs of other advances exist as well, but have not as of yet been shown to signify Svalbard-wide advances larger than that of the late LIA (Miller et al., 2017; Svendsen and Mangerud, 1997; Reusche et al., 2014; Werner, 1993).

The LIA climate on Svalbard has been inferred from both instrumental and proxy records. In addition, historical photographs and illustrations from the last few hundred years reveal glimpses of the state of the archipelago's glaciers. Through lake sediments, it is inferred that the summer air temperatures on Svalbard have been relatively stable during the last 1 800 years (D'Andrea et al., 2012). Ice-core records, on the other hand, infer decadal winter air temperature variations in the order of $5°C$, with a cooling trend between AD800 and the late 1800s, proceeded by rapid step-like winter warming (Divine et al., 2011). Instrumental temperature records from Svalbard Airport show that summer temperatures increased slowly by $0.1°C\ decade^{-1}$ over the 1900s, but spring temperatures varied much more with an increasing trend of $0.4°C\ decade^{-1}$ (Figure 1.3; Nordli et al., 2014). This corresponded to large concurrent variations in sea ice extent in Greenland, suggesting that the large winter variations were not just local to Svalbard (Divine and Dick, 2006). Precipitation trends are more poorly constrained, but measured values from Longyearbyen in 1912–2017 show a statistically significant $3.7\%\ decade^{-1}$ increase trend, and modelled Svalbard-wide precipitation in 1958–2017 suggests an increase by $1.9\%\ decade^{-1}$ (Hanssen-Bauer et al., 2019). Photographs portray many glaciers during the 1800s with land-terminating cliffs (Garwood and Gregory, 1898; Hamberg, 1894; Holmlund and Martinsson, 2016). Such cliffs on land-terminating glaciers are today only found in dry and cold

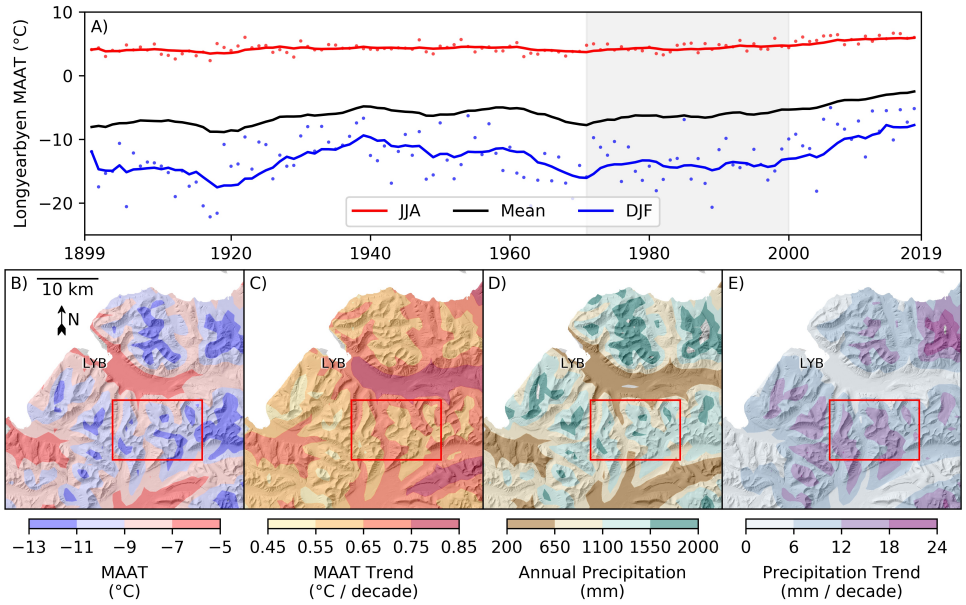

Figure 1.3: The climate near Longyearbyen on Svalbard. **A)** June–July–August (JJA), annual, and December–January–February (DJF) temperature variation from the airport of Longyearbyen (Nordli et al., 2014). The 1971–2000 climate interval marked in grey. **B), C), D)** and **E)** show the concurrent spatial variation of air temperature, precipitation and changes thereof (van Pelt et al., 2019). The location of the study site (Figure 1.4) is outlined in red.

environments such as Antarctica, and on top of Kilimanjaro (Bull and Carnein, 1970; Mölg et al., 2008). These observations are vastly dichotomous to what is observed in photographs from the early 1900s, where most terrestrial glaciers had developed smooth glacier termini and showed strong signs of retreat, although some were contractictibly advancing (De Geer, 1910; Isachsen, 1912). These observations support that Svalbard was a dry and cold environment during the LIA, relative to the warmer and wetter conditions that reign today.

Nordenskiöld Land is part of the Central Tertiary Basin, a geologic sequence of marine, shallow marine, and terrestrial sedimentary deposits (Dallmann, 2007). The constituent layers are almost horizontal near Longyearbyen and the study area, which gives central Spitsbergen its iconic mountains; steep sides with expansive plateau tops and step-like breaks between the two due to differential erosion of the varying geological units. The units in the study area consist of sandstone and mainly of shale, which are loose and enable the production of fine-grained tills when an erosive glacier is present. With the high clay and silt content of the tills, the hydraulic conductivity is low, forcing most of the water to run above instead of within the sediment. This may be part of the explanation for why surges are so common, because low

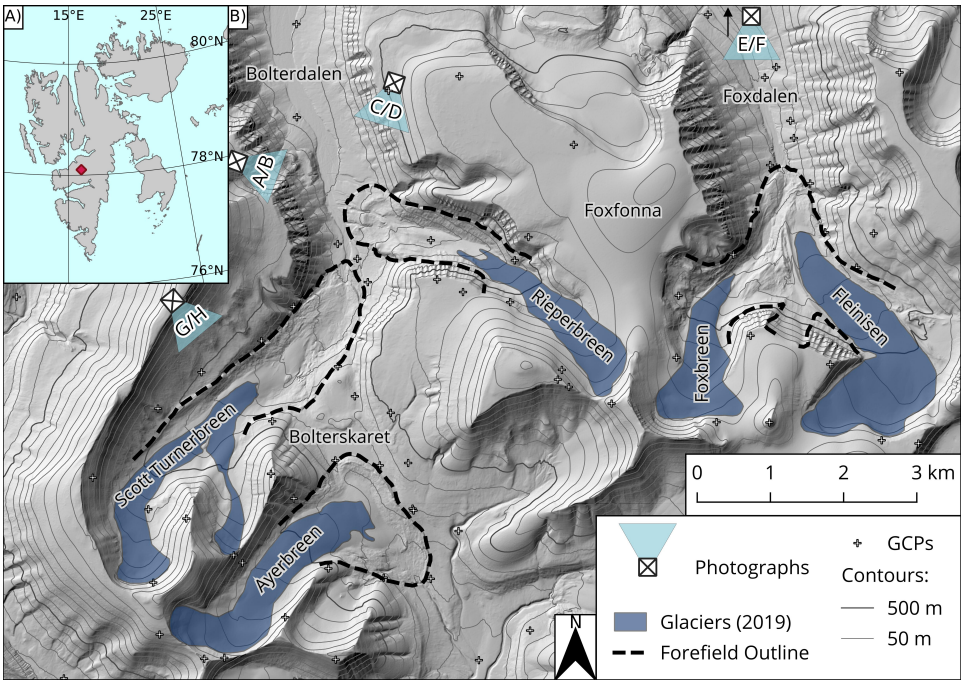

Figure 1.4: A) Location of the study site on Svalbard and **B)** the relative location of the studied glaciers. The photographs with their associated letters are seen in Figure 3.1. Photographs E and F are 7.3 km north of their label.

hydraulic conductivities such as those in Nordenskiöld Land correlate well with observations of surges on Svalbard (Jiskoot et al., 2000).

The climate of Nordenskiöld Land varies largely with altitude and with distance to the western and eastern coasts. Annual precipitation reaches 581 mm w.e. in Barentsburg near the west coast, while Longyearbyen only gets about 196 mm w.e. per year in 1971–2000 (Hanssen-Bauer et al., 2019). At higher elevation, annual precipitation of more than 2000 mm w.e. may occur, which enables a high accumulation rate on glaciers that reach it (Humlum, 2002; van Pelt et al., 2019). The mean annual air temperature generally gets cooler in an easterly direction, being $-5.9°C$ in Longyearbyen, and a modelled $-9.5°C$ on the east coast of Svalbard in 1971–2000 (Hanssen-Bauer et al., 2019). The temperature lapse rate near Longyearbyen varied between -0.4 *to* $-0.6°C/100$ *m* in 2000–2011 (Christiansen et al., 2013), meaning the mean annual air temperature of the study area should have been around -8 *to* $-9°C$ (the mean glacier elevation is 537 m a.s.l.) in 1971–2000. Conclusively, the climate of Nordenskiöld Land has a large variation, and covers the spectrum of both an Arctic desert and a more maritime environment.

2

Theory

To understand why and how a glacier may surge with or without a climatic interference, not just this interplay, but the fundamental drives of a glacier must be thoroughly understood. Here, some of these key concepts are presented to further contextualise the interconnection between climate and glacier dynamics.

2.1 Controls of glacier flow and mass balance

The behaviour of a glacier is a direct reflection of the topography, geology and climate that surrounds it. Therefore, if glaciers and their changes can be understood, deductions about the current and past climate can be made. Temperature has the most direct control over the fate of a glacier, since it linearly scales with ablation and thus meltwater production (Hock, 2003). The availability of water is a deciding factor for a glacier's dynamics; a high availability without proper discharge makes the entire glacier slide over its substrate, yielding order-of-magnitiude increases in ice-flow velocity, whereas a low availability or efficient water discharge causes the glacier to freeze to its bed, considerably restricting its speed (Meier and Post, 1987). The form and amount of precipitation governs the throughput of a glacier's mass, which heavily dictates how it moves. Several metres of snow per year will not only yield a high production of ice, but can also insulate summer meltwater to create perennial firn aquifers that makes the produced ice temperate (near

0°*C*), with considerable inclusions of water (Stenborg, 1970; Östling and Hooke, 1986). They heavily alter the dynamics of a glacier, since they dictate if the produced ice will be warm-based (and thus prone to basal sliding) or not, and thus control a glacier's entire energy balance (Wilson and Flowers, 2013). Firn aquifers are thus common in climates where annual air temperatures reach far below zero, such as in Greenland and Antarctica (Forster et al., 2014; Lingle and Brown, 1987). The same occurrs at higher elevation on Svalbard, where winter accumulation far exceeds summer melt (Sverdrup and Ahlmann, 1935; Schytt, 1969; Björnsson et al., 1996). If too little snow either falls over the winter, or too much of it melts during the summer, perennial firn aquifers may not survive as they are no longer properly insulated. As a consequence, glaciers at lower elevation have gotten colder since the early 1900s, compared to their more temperate past (Björnsson et al., 1996; Bælum and Benn, 2011; Hodgkins et al., 1999; Sevestre et al., 2015). In summary, an elevation-dependent evolution is seen, where some glaciers grow colder with a warming climate, while those at higher elevation may get warmer since precipitation gains can outweigh the warming trend (van Pelt et al., 2016). A changing climate changes the conditions for glaciers all over the world, and their dynamics will as a consequence change as well, which need to be properly understood to project their future.

2.2 Glacier surging

Glacier surges feature a temporary increase in glacier velocity, but to understand their fundamentals further than this, a literature review is needed. The three terms *surges*, *surge-type glaciers* and *surge cyclicity* are often encountered separately or in combination in literature. Glacier surges always refer to the active phase of the surge, and can be observed or later be reconstructed based on geomorphological evidence (Farnsworth et al., 2016; Sevestre and Benn, 2015). What makes a glacier surge-type or not is however more unclear. Most refer to a glacier being surge-type if at least one glacier surge has been identified (e.g. Dowdeswell et al., 1995; Hagen et al., 1993; Jiskoot et al., 2003; Sevestre and Benn, 2015). An alternate explanation is that glacier surges may also occur as one-off events, since most glaciers on Svalbard have only been observed to surge once (Hagen et al., 1993). This addition requires that a reference kind of *surge-type glacier* exists: one that occurrs periodically in a defined surge cycle. Periodic build-up and release of mass is indeed seen in many glaciers all over the world (e.g. Eisen et al., 2001; Kjær et al., 2008; Lovell et al., 2018). Multiple surges at the same glacier have been observed less than a dozen times on Svalbard, which have been interpreted to be part of their natural surge cyclicities (Flink et al., 2015; Larsen et al., 2018; Murray et al., 2003). Multiple observations per glacier are however in the strong minority, and a relevant question to ask is whether or not the glaciers that only surge once really should

be classified as surge-type glaciers? If sporadic surging is allowed within the definition of a surge-type glacier, then perhaps yes, but if a cyclicity is part of the definition, how can cyclicity then be read from a single observation? Today, we are seeing glaciers surge in new areas and new ways, in places where they have not been observed to surge before (Sevestre et al., 2018; Willis et al., 2018). It highlights the need for multiple subclasses of surging glaciers that do not yet exist, for example glaciers with either *cyclic* or *sporadic* surges.

2.2.1 Enthalpy cycling to explain surge cyclicity

Many mechanisms for surging have been suggested over the years, and a theory of unifying these is suggested by Benn (2019) through describing the interplay between mass and enthalpy budgets on glaciers. The enthalpy of a glacier is defined by its basal temperature and water content, where more of this leads to higher enthalpy (Aschwanden et al., 2012). The rates of production and dissipation of enthalpy will heavily dictate the dynamic properties of the glacier, where a high enthalpy system will lead to fast flow, and low enthalpy leads to slow flow. A *normal* glacier has a stable steady-state geometry, while the steady-state of a *surge-type* glacier is unstable (Benn et al., 2019a). These unstable steady-state glaciers cycle between losses and gains of mass and enthalpy, respectively, leading to variations in ice flow velocities. These variations are described with two differential equations. The first is for mass change (height in their one-dimensional example):

$$\frac{dH}{dt} = (\dot{a} - \dot{m}) + \frac{Q_i}{l}, \tag{2.1}$$

where $\dot{a} - \dot{m}$ is the surface mass balance (accumulation rate – ablation rate), and Q_i is the flux of the glacier in relation to its length (l). Second, the change in enthalpy is described as:

$$\frac{dE}{dt} = \tau u + G - q_i + \rho L \beta \dot{m} - \frac{\rho L Q_w}{l}, \tag{2.2}$$

where τu is the strain heating, G is the geothermal heat flux, q_i is the rate of conductive cooling, $\rho L \beta \dot{m}$ is the enthalpy of meltwater reaching the bed, and $\rho L Q_w$ is the subglacial discharge of water in relation to its length (l). These two equations are codependant, e.g. by the ice flux scaling with the total enthalpy, while strain heating and the closure rate of subglacial conduits is highly dependant on the available glacier mass. In certain geometric, geological and climatic settings, these two differential equations never stabilise, but vary

cyclically between high and low enthalpy states, or in other words cyclic surging. The high enthalpy states are according to the model mostly triggered by the exponential rate of meltwater reaching the bed once a considerable ice flow velocity is reached, due to increased crevassing. This model is highly generalised, but it helps in isolating the core drives of glacier surges, and can be built upon to further explain the various triggers and reasons why glaciers can become unstable.

2.2.2 How can climate change affect surging?

The conclusions of Sevestre and Benn (2015), that a "climatic envelope" exists where most glacier surges occur, raises questions about whether or not changes in climate may affect the frequency of surging in the future. The glacier substrate geometry and geology also play major roles, but the importance of the climatic component is that it can change at decadal time-scales. A trigger of many modern glacier surges has been attributed to excessive melt at the terminus, yielding high driving stresses that eventually lead the glacier to collapse forward (Nuth et al., 2019; Sevestre et al., 2018). This kind of surge initiated at the terminus has a clear connection to warming temperatures, but what about the more traditional top-down surge? Benn et al. (2019a) elegantly showed how increasing driving stresses and especially meltwater reaching the bed through crevasses can lead to runaway enthalpy production that triggers a surge. But these two factors are not the only existing enthalpy sources, so an important question is what other surge triggers are possible. Examples of other direct or indirect enthalpy sources are: perennial firn aquifers, moulin meltwater transport, warming through volcanic eruptions, earthquake frictional heating, or suddenly increasing load through either natural mass movements or by anthropogenic dumping. The last example has in fact already been shown to have triggered surges (Jamieson et al., 2015). With the emergence of numerous different surge triggers, the question is no longer if climatic or anthropogenic interferences are factors, but rather how important they are, and what their implications are for future ice-loss projections.

2.3 Geomorphology

Identifying and understanding landforms in a landscape can enable its recent history to be reconstructed. The shape, composition and relative location of these landforms can give vital clues to the processes that have been active, granted that the hypothesised processes are understood well enough. In glacier forefields, the presence or absence of landforms such as moraines, eskers, and streamlined landforms, can enable the deduction of previous glacier extents,

glacial hydrology, and past basal thermal conditions that have dictated where and how much the glacier has moved. To accurately understand the formation process of a landform, the composition of the constituent sediment has to be known. The present composition of a sediment is essentially the product of three things: the material from which it originated, the primary process that transported the sediment to where it is today, and the secondary processes that may have since modified it from its original state. Glaciers generally produce diamictic sediments; with an unsorted internal composition ranging from clay (<0.002 mm) or silt (0.002–0.063 mm) fractions, all the way up to the cobble (63–200 mm) or boulder (>200 mm) fractions (ISO 14688-1, 2002; Flint et al., 1960). Glaciofluvial (running water) processes generally wash out a sediment, relieving it of the finer (clay and silt) fractions, yielding a sorted sediment, relative to the unsorted glacial diamicts. The level of sorting on a sediment is therefore a good indicator of what processes have acted upon it. For example, if a ridge within a glacier forefield is entirely composed of sand (0.063–2 mm), the high level of sorting strongly indicates a glaciofluvial origin, and it may together with its shape and relative location in the forefield possibly be indicative of an esker. If the ridge is composed of diamict, however, it is more likely to have a direct glacial origin. A further clue is the presence of striations on clasts, as this is widely believed to indicate modification at the glacier bed, representing them being grinded against each other under a high overburden pressure (e.g. Agassiz, 1838; Geikie, 1863). Conclusively, by knowing the relative location, shape and sedimentary composition of glacial landforms, deductions about past processes can be made, which together enable the reconstruction of a glacier's past.

2.3.1 Tracing surges with landforms

Observing every glacier surge has historically been impossible as Svalbard is only sparsely populated. Since the advent of large-scale photographic surveying in 1936, and the modern abundant availability of satellite data, observations are now easier to come by (e.g. Benn et al., 2019b; Dowdeswell et al., 1995; Sevestre and Benn, 2015). But tracing the history of glaciers before the observational period instead requires analysis of the tracks that they left behind in the landscape. The occurrence of looped moraines is one indication of rapid changes in ice-flow velocity, which would normally not occur in the absence of a surge (Copland et al., 2011; Paul, 2015). Most surges also develop a unique sequence of conditions; elevated flow and often extensive crevassing, followed by a sudden stagnation in ice-flow and therefore low erosion (Meier and Post, 1969). Landforms indicative of rapid flow can thus be preserved in the landscape, compared to a temperate glacier's retreat where erosion continues, fading its own imprints (Boulton and Paul, 1976). The most obvious indicator of high flow followed by rapid stagnation is the preservation of crevasse-squeeze ridges

(CSRs; Sharp, 1985). They are largely believed to form through basal infill of crevasses, and only seem to be preserved if the glacier stagnates and retreats without further basal movement, a sequence which is almost unique to a glacier surge. The only other scenario where similar ridges can be preserved seems to be when ice-streams stagnate rapidly (Evans et al., 2016). In smaller systems, however, surging is the uncontested formation process for CSRs. Since these ridges are often prominent from a distance, they can be used to remotely identify glacier surges long after they happened (e.g. Farnsworth et al., 2016). But care should still be taken, as they can be morphologically similar to ridges formed through supraglacial infill of crevasses or sparse retreat moraines, and their internal structure should optimally be checked before concluding their genesis.

3

Methods

Two scopes were analysed in this study: a global analysis of the present and possible future occurrences of glacier surges, building on the work by Sevestre and Benn (2015), and a detailed case study of five glaciers in Bolterdalen and Foxdalen on Svalbard. The latter have been studied using aerial image and drone photogrammetry, geomorphological mapping, ground penetrating radar surveying, and interpretation of historic observations. Together, the methods enable a comprehensive timeline of each glacier to be reconstructed, which sheds light on when and why they may have surged.

3.1 Global surge occurrence analysis

Svalbard has an unusually high frequency of observed surges, and clues for why may lie in the climatic, geological, and topographic setting of the archipelago. Sevestre and Benn (2015) unprecedentedly showed that global observations of glacier surges are clustered within specific geometric and climatic conditions. The climatic component is especially interesting, as we currently experience rapid changes in it, and tendencies of regions to surge may thus change, for the better or worse. The climatic settings by Sevestre and Benn (2015) were extracted from the ERA-1 reanalysis dataset, with a spatial resolution of 0.75° x 0.75° between January 2000 and December 2009. The most recent reanalysis product, ERA-5, gives values back to 1979, and a 41 year window (1979–2019) of climate data is now available (Copernicus Climate Change

Service, 2019). Therefore, climatic trends can be assessed, to further shed light on the past and future of surging.

Points representing every glacier in the RGI database (RGI, 2017), containing the surging or non-surging information provided by Sevestre and Benn (2015), were compared to the global ERA-5 1979–2019 climate and trend, by picking the values of the nearest 0.25° x 0.25° pixel. Their observational uncertainties are marked as either confirmed (1), very probable (2) or possible (3), and only the two most certain (1–2) categories were used here. Another noteworthy source of error in the surge database is the timing spread from 1861 to 2013, which makes it impossible to pinpoint the exact climatic setting for each surge. Due to the indicative rather than exact nature of the ERA-5 climate data, however, the uncertainty in surge-timing is not treated as a bottleneck here, but it should be considered for future work. Since the climate of Svalbard was assumed to contribute to its high surge-frequency, other areas with a similar climate were identified (Figure 1.1). The *Svalbard climate* range was estimated using the mean and standard deviation of each ERA5 pixel representing the archipelago, yielding a precipitation and temperature range of 466 to 662 mm w.e. and $-10.1°C$ to $-6.6°C$, respectively. Areas projected to reach this *Svalbard climate* before 2100 and 2200 were then estimated by extrapolating the climatic trends of 1979–2019. Worth noting is that the future projections consider a constant rate of change, but in reality the rate seems to be accelerating, meaning that distant projections (e.g. 2200) may actually be closer in time than what is estimated.

3.2 Photogrammetry and drone surveying

Aerial image surveys have been performed by the Norwegian Polar Institute (NPI) over Bolterdalen, Foxdalen and the neighbouring areas in 1936, 1961, 1990 and 2009, which were used here to reconstruct the past shape, extent, and volume of the studied glaciers. The southernmost kilometre of Scott Turnerbreen and Ayerbreen was covered in 2011 instead of 2009, but topographic profiles over this seam show offsets of less than a metre, and was for simplicity therefore treated as only the year 2009. Since the 2009 survey was 11 years old as of the time of writing, a more current timestamp of geometry was sought. This was solved with oblique drone surveying, by taking pictures along the mountain sides of all the studied glaciers. The forefields of each glacier were also covered with vertical drone surveys, allowing for high-resolution geomorphological mapping. Photogrammetric reconstructions were performed in Agisoft Metashape 1.5, and parameters of each survey are shown in Table 3.1.

Ground control points (GCPs) were derived from the orthomosaic and DEM

Table 3.1: Parameters of the photogrammetric reconstructions. A DJI Phantom 4 Pro was used for the 2017–2018 surveys, and a DJI Mavic 2 Pro was used for the 2019 surveys. The DEM Resolution was chosen in order to cover a sufficient amount of points (DEM Population), and therefore varies slightly among the surveys. The ground sample distance (GSD) is the recommended orthomosaic resolution in Metashape.

Survey name/type	Vertical images	Oblique images	GCPs	$RMSE_x$ (m)	$RMSE_y$ (m)	$RMSE_z$ (m)
Aerial surveys						
NPI 1936	24	-	25	1.56	1.78	1.26
NPI 1961	6	-	32	0.65	0.67	0.97
NPI 1990	90	-	40	0.58	0.40	0.89
Drone glacier surveys						
Ayerbreen (2019)	-	53	7	1.16	0.85	0.72
Scott Turnerbreen (2019)	-	99	8	1.31	0.54	0.94
Rieperbreen (2019)	-	164	10	0.45	0.39	0.59
Foxdalen (2019)	-	140	8	0.29	0.67	0.87
Drone forefield surveys						
Ayerbreen (2018)	607	87	5	0.22	0.15	0.55
Ayerbreen Ridges (2019)	148	18	7	0.73	0.63	0.53
Scott Turnerbreen (2018)	643	105	6	0.49	0.59	1.30
Rieperbreen (2017)	724	145	5	0.15	0.11	0.13
Foxdalen (2018)	198	42	5	0.35	0.29	1.29

from 2009 that has already been processed (Norwegian Polar Institute, 2014). Deriving ground control from a reference data set instead of from a differential GNSS in the field is more uncertain, but a higher quantity of GCPs can be collected. It is thus advantageous in respect to quantity over quality, when compared to the field-based approach (Girod et al., 2018; Hong et al., 2006; Holmlund and Holmlund, 2019; Mertes et al., 2017). Since the reference elevation data were quite coarse (5x5 m), an error estimate of the GCP placement was needed. By sub-sampling the high resolution 21 cm/px DEM from the forefield of Scott Turnerbreen to a 5 m/px grid, the resultant standard deviation between these two products was 0.3 m. This error was assumed to be representative for the rest of the study area, and was subsequently used as the GCP accuracy in Metashape.

Volume change was calculated by subtracting two DEMs with each other, and multiplying the resultant mean elevation change within the maximum covering glacier extent with the respective area. Lengths were calculated from the mean of 20 glacier transects with a spacing of 10 m around the glacier centrelines.

Table 3.1: (Continued)

Survey name/type	Dense Quality	Dense Filtering	Dense Count	DEM Res. (m/px)	DEM Pop. (pt/px)	GSD (cm/px)
Aerial surveys						
NPI 1936	High	Mild	29,596,040	50	253	117.0
NPI 1961	High	Aggressive	123,864,881	10	72	60.3
NPI 1990	High	Aggressive	882,290,896	10	578	20.3
Drone glacier surveys						
Ayerbreen (2019)	U-High	Aggressive	121,168,194	5	492	23.6
Scott Turnerbreen (2019)	U-High	Aggressive	80,831,776	5	361	30.1
Rieperbreen (2019)	High	Aggressive	60,831,855	5	351	15.6
Foxdalen (2019)	High	Aggressive	66,310,165	5	160	21.5
Drone forefield surveys						
Ayerbreen (2018)	High	Aggressive	177,324,943	0.12	9.4	7.1
Ayerbreen Ridges (2019)	U-High	Aggressive	329,310,339	0.014	70.2	1.2
Scott Turnerbreen (2018)	High	Aggressive	11,974,822	0.21	1.2	10.5
Rieperbreen (2017)	High	Aggressive	87,352,626	0.18	8.3	8.8
Foxdalen (2018)	High	Aggressive	25,796,867	0.33	4.3	16.4

3.3 Historical observation and imagery

Quantitative data before the aerial surveys in 1936 are much harder to come by, but unlike many other remote glacierised areas, observations from early explorers often exist from Svalbard. This is the case for Bolterdalen and Foxdalen, whose first known and recorded visit was in 1896 by explorer Martin Conway, and geologists Edmund Garwood and John Gregory (Conway, 1897; Garwood and Gregory, 1898; Gregory et al., 1897). These works are filled with both empirical observation and a sparse selection of photographs, which give numerous clues about the state of the glaciers in Bolterdalen and Foxdalen during the late 1800s. While these observations provide qualitative data at best, the boundary between observation and interpretation is clear in these publications, and were therefore seen as reliable sources of information.

Certain small observational details can tell a whole story when interpreted correctly. For example, smaller glaciers on Svalbard seldom display extensive crevassing, except when they are surging, since almost all small glaciers are cold-based (Bælum and Benn, 2011; Björnsson, 1981; Hodgkins et al., 1999; Sevestre et al., 2015). Therefore, if a glacier is described as being heavily crevassed and this does not correspond to excessive undulations in its basal topography, it can be safely assumed to surge during the time of observation. If, however, a glacier is easily traversed, major crevassing like that seen on Scott Turnerbreen in 1914 (Figure 3.1G) is unlikely, and the glacier is most likely not surging at

the moment. Historic observations can thus yield a useful collection of clues, which help to put the subsequent quantitative data in perspective.

Less uncertain are interpretations made here from the 1914 photographs taken by Adolf Hoel, which are currently archived by the National Library of Norway. These were taken as part of a larger campaign to map most of Svalbard, for strategic, resource and exploratory purposes (Barr, 2009). In other areas on Svalbard, the large quantity of historic photographs allow photogrammetric reconstructions of glaciers in the early 1900s (Holmlund, in review), but the overlap of photographs in this area were unfortunately not high enough for current photogrammetric software to use. By simply observing the surficial appearance of a glacier, however, its current state can be safely determined, which then ties well together with subsequent quantitative data. By also revisiting the places where these photographs were taken, they were recaptured, giving both a visual and quantitative perspective on how much and where the glaciers have changed. The modern and historic photographs were overlaid by stretching them to fit each other exactly in Adobe Photoshop CC 2019, so that the past glacier extents could be delineated, showing where in the landscape that corresponds to today (Figure 3.1). Details such as rocks and snowfields were then used to digitise the extents in modern orthoimagery. Here, the high-resolution drone surveys gave an excellent spatial reference to digitise the extents, which could then be used to measure areal and length changes.

3.4 Geomorphological mapping

Geomorphological mapping was predominantly made from the high-resolution (1–33 cm/px) orthomosaics and DEMs available from the drone-surveys. To match the surficial expression of the landforms with their internal composition, many landforms were also examined in the field. Fieldwork was carried out multiple times per year between 2016 and 2019, but on 21 August 2019, the

Figure 3.1: Historic photographs, and their modern counterparts, all taken in late July. Shown are Rieperbreen (**A**, **B**), Scott Turnerbreen (foreground; **C**, **D**, **G**, **H**), Ayerbreen (background; **C**, **D**, **G**, **H**) as well as Fleinisen (left; **E**, **F**) and Foxbreen (right; **E**, **F**). The 1914 photographs were taken by Adolf Hoel, photograph **F** was taken by Sindre Kolbjørnsgaard, and the other 2019 photographs were taken by the author. The 1914 glacier extents are shown in the 2019 photographs (dashed red), which were later georeferenced by comparing with modern orthomosaics (Figure 4.2).

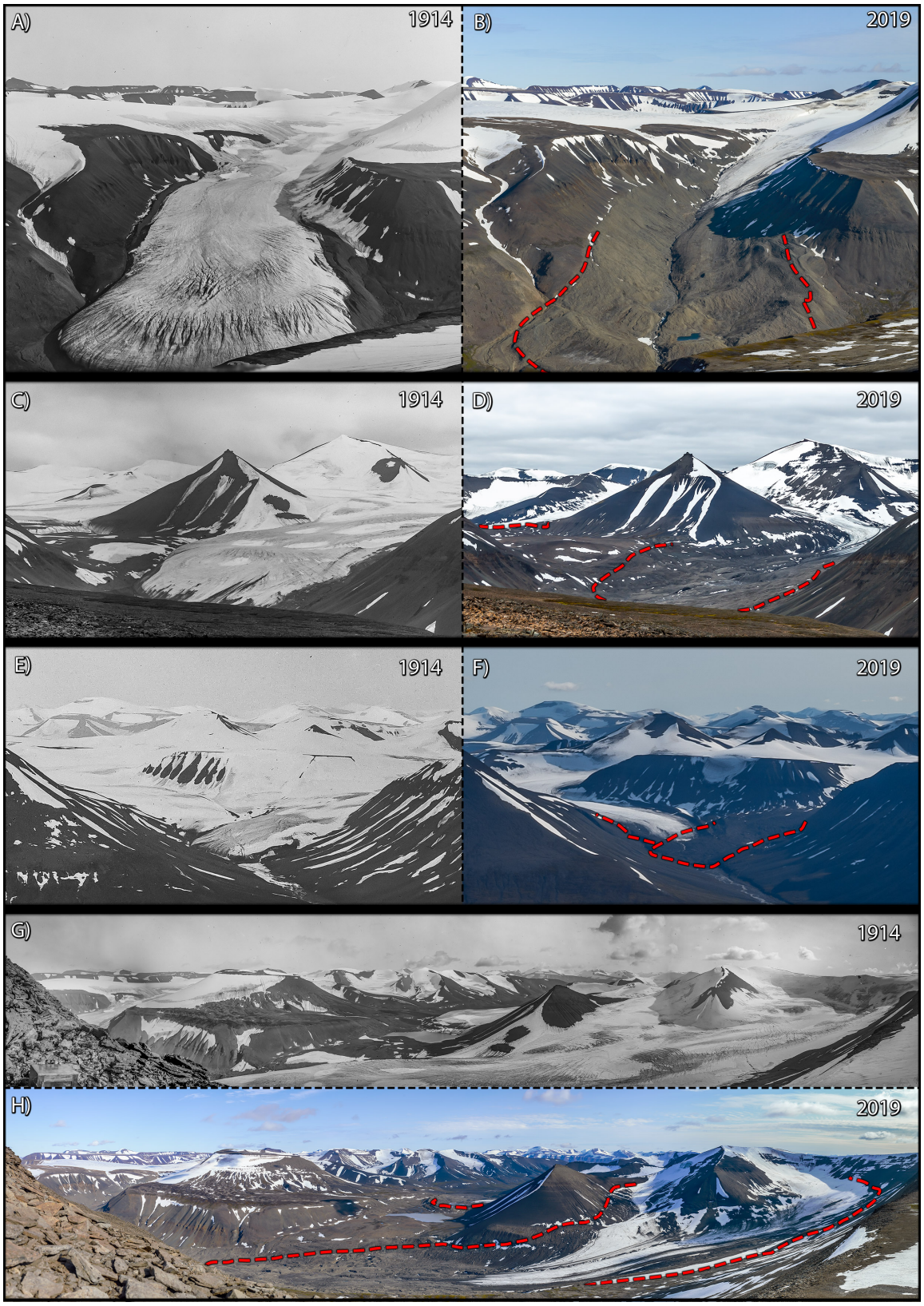
A)
1914
B)
2019
C)
1914
D)
2019
E)
1914
F)
2019
G)
1914
H)
2019

localities in Bolterdalen were systematically revisited and key observations were noted (Table 4.2). These included ground-truthing of sediment composition and internal structure by digging into select landforms, and revision of the remotely classified landform boundaries. In addition, a detail study was performed near the terminus of Ayerbreen to further explain the different 0.5–1 m high ridges that were currently melting out of the ice. The resulting observations made in the field thus allowed for a more certain extrapolation of landform interpretations that were only observed remotely, and assumptions about their genesis and significance for the history of the glaciers could be made more safely.

3.5 Ground penetrating radar and depth interpolation

Between 31 January and 20 February 2019, Rieperbreen, Scott Turnerbreen, Ayerbreen and Fleinisen were surveyed using a Ground Penetrating Radar (GPR). A Malå radar system was used, with a Malå XV monitor and a ProEx Professional Explorer control unit with a generic single-frequency GNSS receiver, dragging an unshielded "rough-terrain" 100 MHz antenna behind a snowmobile going ~15 km/h. Due to time constraints, avalanche and glacier hazards, and equipment limitations in ca. $-30°C$ weather, only centreline surveys were performed. Foxbreen was not covered, as its surrounding was considered too steep to cross, and its partly crevassed surface too dangerous to traverse. Post-processing of the surveys were done in RGPR (Huber and Hans, 2018), using the following filters in succession: DC-shift, timeo-correction, dewow, LF-bandpass, power-gain, topographic Kirchhoff migration (Dujardin and Bano, 2013) and topographic correction. A constant dry-ice velocity of 0.168 m/ns was used for the return time to depth correction (Robin, 1975). The surveys provided invaluable data on interiors of the glaciers, but due to only having partial or lacking glacier coverage, a complementary glacier thickness calculation was sought.

A Svalbard-wide glacier thickness estimation map is available (SVIFT 1.1), made using thickness modelling from glacier surface properties, calibrated with over 8 700 km of glacier depth measurements (version 1.1 available at www.npolar.no; Fürst et al., 2018). This model has a reported error of around 9 m on larger glaciers, but it struggles with smaller glaciers. Compared to the GPR tracks in this study, the SVIFT 1.1 dataset showed no correlation (r=0.26). A modelling approach was however still needed to get a feasible result, since the glacier centreline surveys were not considered to cover enough of the glaciers, especially on Fleinisen where the interpolation distance would reach up to 800

m. Therefore, a simplified thickness model was constructed, inspired by the methodology for the SVIFT dataset (Fürst et al., 2017).

Based on experimentation, the slope, elevation, and elevation change were found together to correlate with ice thickness. Therefore, a multi-variable linear relation was constructed, and trained using the available depth data from the study area:

$$H(\alpha, Z, dH \cdot dt^{-1}) = a \cdot \alpha + b \cdot Z + c \cdot dH \cdot dt^{-1} + d, \tag{3.1}$$

where a, b, c and d are constants to solve for, α is the slope angle in degrees of the ice surface at a specific point, Z is the respective elevation of the ice surface, and $dH \cdot dt^{-1}$ is the yearly surface elevation change (2009–2019) at the point. Since the aim was a general non-glacier specific relationship between these parameters, data from all the surveyed glaciers were used in the same model training, thus reducing the risk of overfitting. The correlation resulted in many outliers, so Random sample consensus (RANSAC) regression was used to find the general trend. The best solution for Equation 3.1 gave an RMSE of 16.9 m, which was subsequently used as the error for the unconstrained model. The model gave plausible results for the glacier body, but near the edges, the glacier thickness did not eventually reach zero, since no parameter was yet used to signify the terminus proximity. In addition to this, a term was also needed to only allow positive thickness values, as the model had a tendency to produce negative outliers near areas with noisy elevation change data. These two corrections were added using the following equation:

$$H_{model} = max\,(H, 0) \cdot min\left(\frac{D}{100}, 1\right), \tag{3.2}$$

where H is the uncorrected thickness model (Equation 3.1) and D is the nearest distance to the glacier margin (thickness should be zero when $D = 0\ m$, and is unaffected when $D > 100\ m$). Due to the generalising nature of the model, estimated values near the centreline deviated from the measured values (by the model RMSE of 16.9 m). This was corrected for by generating a spatially interpolated model vs. measured offset field along the glacier (measuring zero at the margins) and then subtracting the offset with the modelled glacier thicknesses.

$$H_{corrected}(x, y) = H_{model}(x, y) - H_{offset}(x, y), \tag{3.3}$$

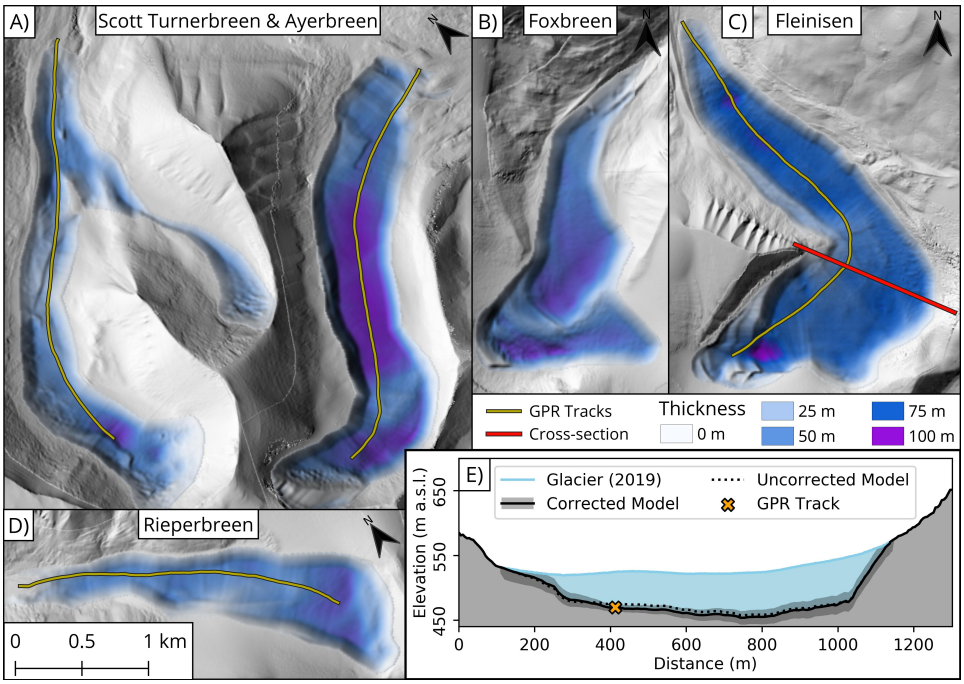

Figure 3.2: **A), B), C)** and **D)** Thickness fields from the model developed in this study, based on GPR tracks on the studied glaciers. Note that the bed of Foxbreen (**B**) was not surveyed, and is purely based on the model output. **E)** Cross-section of Fleinisen, showing the difference between the uncorrected and corrected depth model from west to east, and the uncertainty of the estimation. The vertical axis is exaggerated by five times.

The corrected model resulted in spatially complete thickness maps, that fit the exact values of the measured data (Figure 3.2).

3.6 Error calculation

Many sources of quantitative and qualitative error are present in this study, and are discussed throughout the text. How the quantitative sources of error were calculated are shown here.

3.6.1 Depth modelling error

The glacier depth model provided a spatially complete estimation of glacier thicknesses, but this is naturally not without uncertainty. The estimated glacier depth error must vary depending on the proximity to a measured value.

Therefore, the total depth error for each glacier was calculated by the average of an interpolated error field within each glacier's 2019 extent. The error at the glacier boundary was given a value of 16.9 m, corresponding to the associated RMSE of the unconstrained model, whereas places where data existed were given the GPR manufacturer error of ±5 m. All areas between the boundary and the GPR tracks were then linearly interpolated, and the average of this error was used estimated for each glacier separately. Thickness errors for the glaciers in the past were for simplicity calculated by assuming that the terrain they once covered is relatively unchanged, and thus do not contribute to the uncertainty. This assumption was incorporated by scaling the interpolation error with the size of the glacier surface relative to 2019, yielding smaller errors for larger areas:

$$\epsilon_D = \frac{A_{2019}}{A} \cdot \epsilon_{D_{2019}}, \tag{3.4}$$

where ϵ_D is the depth interpolation error for each respective glacier, A_{2019} is the 2019 area, A is the area for each respective year, and $\epsilon_{D_{2019}}$ is the depth interpolation error within the 2019 boundary.

3.6.2 Glacier thickness and volume error

Elevation change errors were calculated by taking the Pythagorean distance of the vertical RMSEs of the two compared models (Table 3.1). The total thickness error was then calculated from a combination of photogrammetric and thickness interpolation errors (Table 4.1):

$$\epsilon_T = \epsilon_D + \sqrt{\epsilon_Z^2 + \epsilon_{Z_{2019}}^2}, \tag{3.5}$$

where ϵ_T is the error in glacier thickness for a specific year, $\epsilon_{D_{2019}}$ is the associated depth interpolation error, and ϵ_Z is the associated photogrammetric $RMSE_z$ (Table 3.1). Volume errors were subsequently calculated by multiplying each year's and glacier's respective thickness error with its area.

4

Results

4.1 Global surge occurrence analysis

The glaciers of Svalbard show an unusually high tendency to surge, and the climate of the archipelago seems to be at least part of the explanation for why (Figure 1.1; Sevestre and Benn, 2015). Furthermore, observations and inferences indicate that surging was more common in the late LIA than they are today (Figure 1.2; Dowdeswell et al., 1995; Ottesen et al., 2017; Nuth et al., 2019; Sevestre et al., 2015). Changes in temperature and precipitation on many Arctic, Himalayan and Antarctic regions have weak or strong trends toward the approximate climate that Svalbard has today, and an important question is whether or not this will affect the tendency of these regions' glaciers to surge. Examples of areas that may reach a *Svalbard climate* are Servernaya Zemlya, whose largest ice-cap just recently started surging (Willis et al., 2018), and Northeast Greenland where some surges are already recorded (Mouginot et al., 2018). Glaciers in Eastern Greenland, further south of the exemplified area, seem to have a similar tendency to surge compared to Svalbard (Jiskoot et al., 2003), so seeing this phenomenon spread in Greenland is possible.

4.2 Bolterdalen and Foxdalen

Direct or indirect inferences of the five studied glaciers on Svalbard show that four of them seemed to have surged between around 1896 and 1936. However,

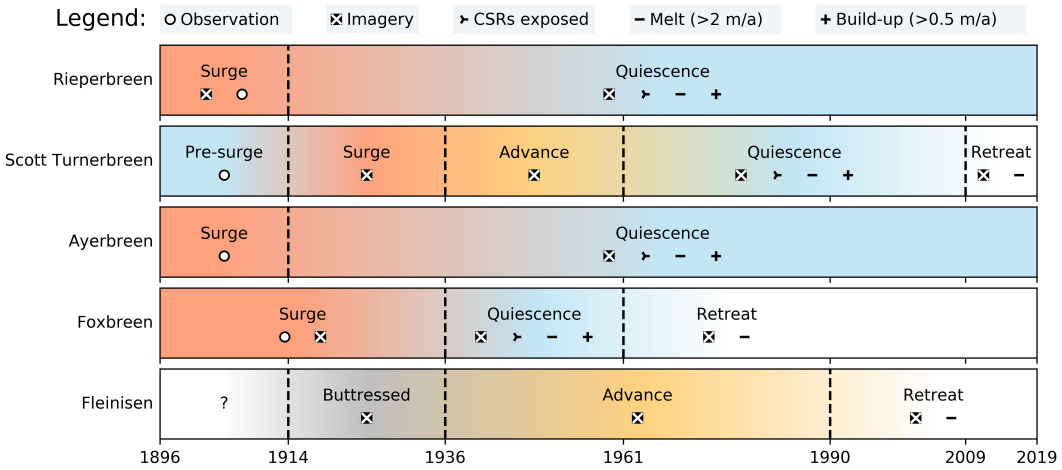

Figure 4.1: Interpreted timelines of the studied glaciers. Warm colours indicate advances while the cooler colours indicate retreat or stand-stills. The name of an interval (divided by dashed lines) was chosen based on the data that supports it. Interpretations based on observation refer to those made from literature (Conway, 1897; Garwood and Gregory, 1898). CSRs exposed in the forefield were used as a sign of past or current surge-phase quiescence. Excessive melt rates (above 2 m/a) and accumulation zone build-up (above 0.5 m/a) were together considered additional indicators of quiescence, compared to regular retreat which would not indicate a surge-type behaviour.

they all seem to be cold-based today, indicated by the bottom being clearly visible throughout the GPR surveys (c.f. Björnsson et al., 1996; Dowdeswell et al., 1984) The photogrammetric, observational and geomorphological data that build this timeline are summarised in Figure 4.1.

4.2.1 Photogrammetry

On average, the studied glaciers lost 77.4%±7.7% of their volumes, or 1094.3± $33.4 \cdot 10^6$ m^3 in total, between 1936 and 2019. Furthermore, they lost about half of their areal extent on average during the same period (Figure 4.2). Fleinisen; the only glacier that showed no signs of surging, consequently lost only half as much as the other glaciers that all showed signs. While comparing one glacier to four others is not statistically significant for all of Svalbard's glaciers, it still highlights the immense need for studying further how surges affect melt-rates in rapid climate change.

Scott Turnerbreen lost the most out of the glaciers in the study area, with a reduction of 91% ± 5%, or $369.5 \pm 36.9 \cdot 10^6$ m^3, between 1936 and 2019. The glacier advanced by 329 m in 1914–1936, and further by 75 m in 1936–1961,

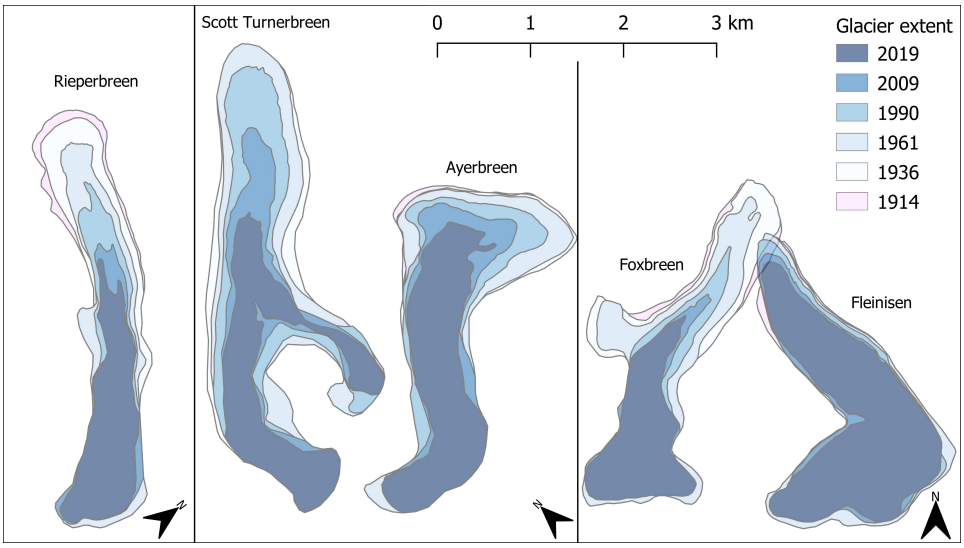

Figure 4.2: Variation in extent of the studied glaciers between 1914 and 2019.

after which it started to retreat (Figures 4.3, 4.4, 4.5). Attributing this entire advance period to one surge sets its duration to somewhere between 22 and 47 years, which is exceptionally long for a surge on Svalbard, where the longest recorded surge to date lasted for ten years (Dowdeswell et al., 1991). Its length may even be described as *too long*, which is discussed later as it may explain why the glacier lost so much of its volume.

While all glaciers in the study area lost considerable parts of their volume in the 1900s, most of them on the other hand gained in thickness at higher elevation (Figure 4.3). This occurrence seemed predominantly elevation based, as it only occurred at the glaciers' upper parts, but it must also have been highly dependent upon the local topography. Foxbreen gained in thickness at as low as 500 m a.s.l., compared to the others that gained above *ca.* 650 *m a.s.l*, maybe due to its numerous north-facing slopes, while Fleinisen showed no positive thickness change whatsoever despite reaching approximately 730 m a.s.l. Local topography may only be part of the explanation, as divergence and emergence velocities are not known here, and a possible high relative flux at Fleinisen might explain why the added mass might not have accumulated like on the other glaciers. Large positive change was seen during the 1900s, especially in the 1961–1990 snapshot (Figure 4.3). Comparing to today (2009–2019), however, it seems to be a reducing trend, but positive thickness rates still reach up to 0.4 m/a on Foxbreen and Ayerbreen.

Results indicate that Fleinisen was the only glacier that did not surge in the study area, but its history is not as simple as an ideal non-surging reference should be, because it also advanced for reasons only indirectly connected to

Table 4.1: The changing geometric properties of the studied glaciers. Elevation change (ΔH) is compared to the antecedent year. The volume fraction that compared to 1936.

Glacier	Year	Area (km^2)	Volume (10^6 m^2)	Volume (%)	Length (km)	Slope (°)	Thickness (m)	ΔH (m)
Rieperbreen	1936	2.7	215.0 ± 17.6	100.0 ± 8.2	4.6	11.1	78.7 ± 6.4	—
	1961	2.2	127.5 ± 16.3	59.3 ± 7.6	4.3	12.2	57.9 ± 7.4	−20.9 ± 1.6
	1990	1.7	78.9 ± 15.5	36.7 ± 7.2	3.7	11.9	47.7 ± 9.4	−10.2 ± 1.3
	2009	1.3	49.8 ± 14.6	23.2 ± 6.8	3.1	12.7	36.9 ± 10.8	−10.8 ± 0.9
	2019	1.2	37.4 ± 13.8	17.4 ± 6.4	2.7	13.0	32.2 ± 11.9	−4.6 ± 0.6
Scott Turnerbreen	1936	4.7	408.0 ± 29.5	100.0 ± 7.2	5.2	9.3	86.8 ± 6.3	—
	1961	4.4	296.7 ± 28.0	72.7 ± 6.9	5.3	9.7	67.8 ± 6.4	−19.0 ± 1.6
	1990	3.4	165.6 ± 26.5	40.6 ± 6.5	5.0	9.7	48.8 ± 7.8	−19.0 ± 1.3
	2009	2.3	80.4 ± 24.3	19.7 ± 6.0	4.2	10.4	34.9 ± 10.6	−13.9 ± 0.9
	2019	1.7	38.5 ± 22.1	9.4 ± 5.4	3.3	11.7	23.2 ± 13.3	−11.8 ± 0.9
Ayerbreen	1936	3.5	297.8 ± 25.8	100.0 ± 8.7	4.6	9.2	86.3 ± 7.5	—
	1961	3.4	251.0 ± 24.8	84.3 ± 8.3	4.6	9.1	74.7 ± 7.4	−11.6 ± 1.6
	1990	2.7	164.1 ± 23.9	55.1 ± 8.0	4.3	8.5	60.4 ± 8.8	−14.3 ± 1.3
	2009	2.2	113.9 ± 22.4	38.2 ± 7.5	4.0	8.9	50.7 ± 10.0	−9.8 ± 0.9
	2019	1.8	79.8 ± 20.8	26.8 ± 7.0	3.6	9.4	45.1 ± 11.8	−5.5 ± 0.7
Foxbreen	1936	2.8	203.5 ± 23.3	100.0 ± 11.4	3.8	11.6	73.8 ± 8.4	—
	1961	2.3	139.8 ± 22.1	68.7 ± 10.9	3.5	11.4	61.2 ± 9.7	−12.5 ± 1.6
	1990	1.5	78.4 ± 20.9	38.5 ± 10.3	2.7	10.7	52.6 ± 14.1	−8.6 ± 1.3
	2009	1.2	54.6 ± 20.2	26.8 ± 9.9	2.1	11.3	44.6 ± 16.4	−8.1 ± 0.9
	2019	1.1	44.2 ± 19.1	21.7 ± 9.4	1.8	11.6	39.1 ± 16.9	−5.4 ± 0.9
Fleinisen	1936	3.1	288.0 ± 33.8	100.0 ± 11.7	3.6	8.6	92.3 ± 10.8	—
	1961	3.1	257.0 ± 33.1	89.2 ± 11.5	3.7	9.2	82.1 ± 10.6	−10.2 ± 1.6
	1990	2.9	197.0 ± 32.6	68.4 ± 11.3	3.6	8.7	68.5 ± 11.3	−13.6 ± 1.3
	2009	2.7	151.3 ± 31.4	52.5 ± 10.9	3.5	9.1	55.7 ± 11.6	−12.8 ± 0.9
	2019	2.5	118.1 ± 29.1	41.0 ± 10.1	3.3	9.0	47.1 ± 11.6	−8.6 ± 0.9

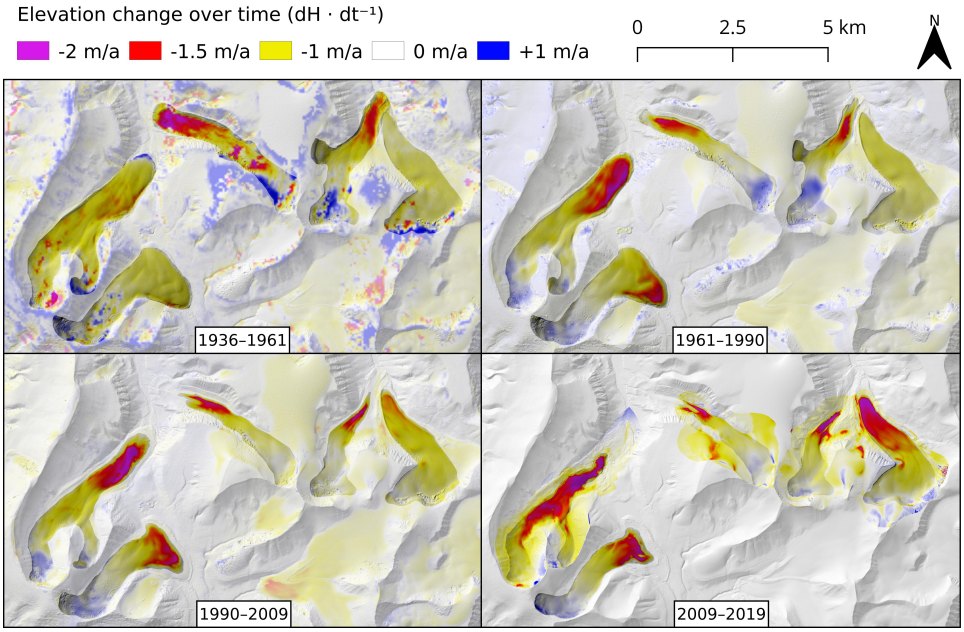

Figure 4.3: Elevation change between 1936 and 2019. The area outside of the studied glacier extents is whited out for increased readability. The lack of colour outside the glaciers in 2009–2019 is due to the targeted coverage of the drone surveys.

climate change. In 1936 and before, the neighbouring Foxbreen covered the otherwise natural path for Fleinisen to extend after having recently surged (Figures 3.1, 4.2). This created a buttressing effect, and as Foxbreen quickly retreated in the latter part of the 1900s, Fleinisen continued to advance until sometime between 1961 and 1990 (Figure 4.4). After 1990, the glacier is now also in retreat, and seems to be losing volume at an accelerating pace.

4.2.2 Historic observation

William Conway and Edmund Garwood traversed both Bolterdalen and Foxdalen in 1896, noting direct or indirect clues for the state of the glaciers they passed (Conway, 1897; Garwood and Gregory, 1898). While ascending one of the neighbouring peaks of Rieperbreen, they had trouble crossing the “maze of crevasses” that covered the surface of the glacier’s upper parts. Signs of extensive crevassing were not visible in 1914 nor in 1936, strongly suggesting that they observed an active surge, or its recent aftermath. They also crossed Foxdalen toward Bolterskaret, which required them to traverse the surface of Foxbreen. Surprisingly, they did this while only mentioning a difficult bergschrund, in spite of the glacier displaying a troublesome crevassed surface

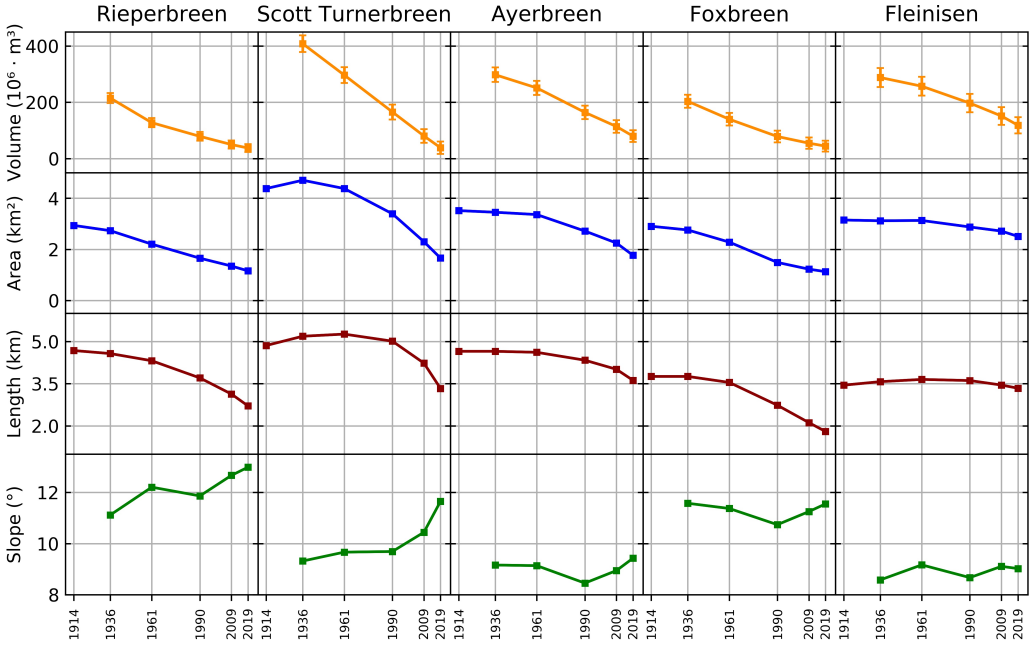

Figure 4.4: Glacier properties.

in 1914. While the lack of a complaint is not usually reliable evidence, they did complain about almost every other part of their journey. Therefore, if the glacier surged sometime between 1896 and 1914, it would be the simplest explanation for this otherwise contradictory evidence. On their way back, Conway and Garwood passed Ayerbreen, and noted its "unusually steep" front which "bulged over in a threatening manner". It is unclear what they meant by this, but combined with the abundance of CSRs in its currently exposed forefield, and subsequent surge-indicative geometric changes, it could mean that they observed it surging. Later, they passed Scott Turnerbreen without a mention, which had probably not yet started surging, and they finally passed the front of Rieperbreen. It was "apparently advancing", and they spent hours noting "The interesting phenomena of the Rieper Glacier's snout", but did not say what this meant. A figure of its terminus (Pl. XIII, Fig. 2 in Garwood and Gregory, 1898) does however show a vertical terminus with ice calving off it. This supports the earlier idea that they caught it in an active surge-phase. After the traverses of Bolterdalen and Foxdalen, Garwood and Gregory (1898) continued to observe and describe multiple glacier surges further east, which was occasionally compared to their aforementioned observations. This is an

Figure 4.5: Glacier profiles. The same horizontal and vertical scale has been used in all plots, with an eight times vertical exaggeration.

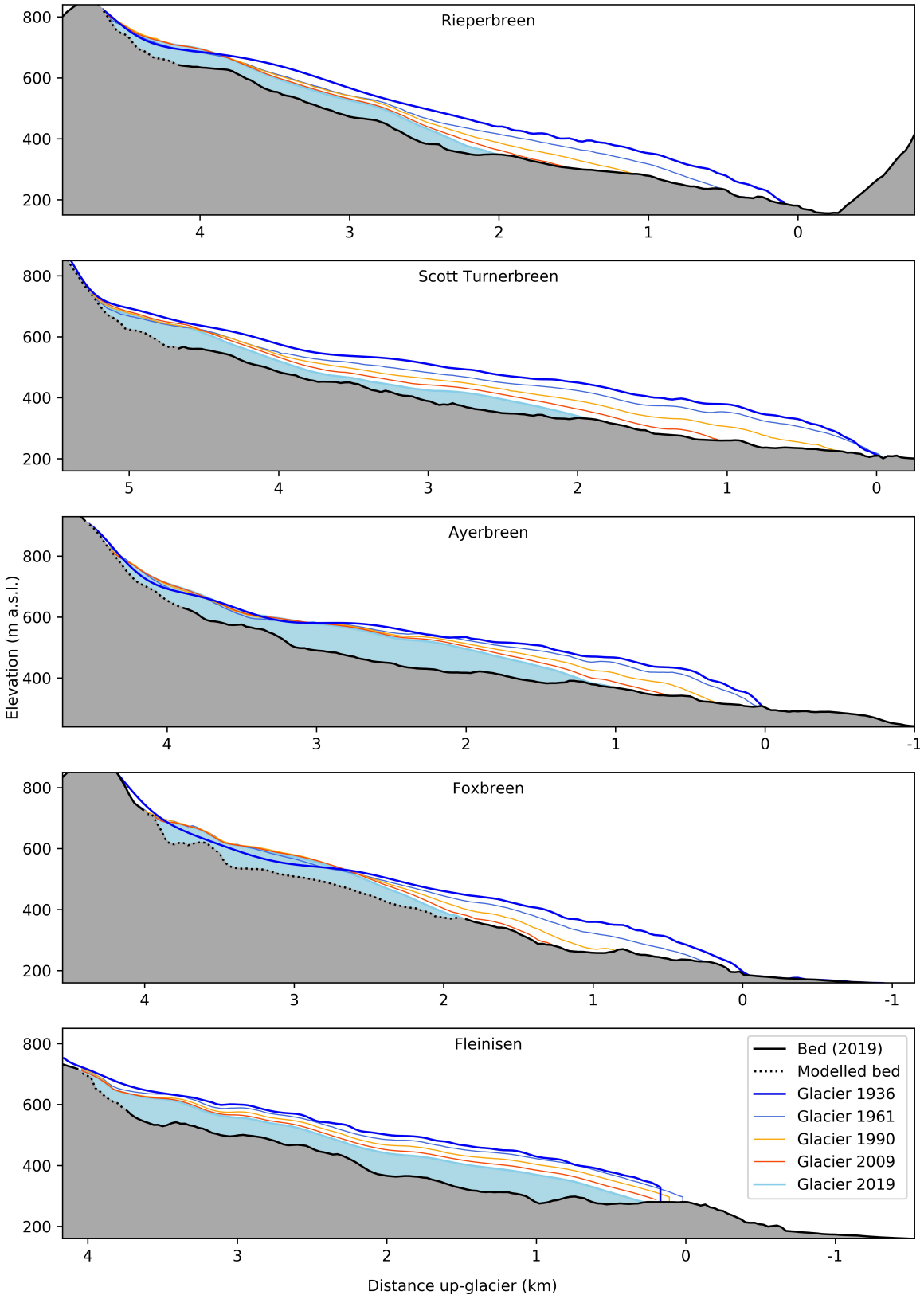
Rieperbreen
Scott Turnerbreen
Ayerbreen
Foxbreen
Fleinisen
Elevation (m a.s.l.)
Distance up-glacier (km)
Bed (2019)
Modelled bed
Glacier 1936
Glacier 1961
Glacier 1990
Glacier 2009
Glacier 2019

important detail, as they obviously understood the phenomenon of glacier surges, and their notes or lack thereof could be seen as reliable.

No other known historic written observations exist, but the photographs taken by Adolf Hoel in 1914 tell an intricate story by themselves. Rieperbreen had bands of crevasses that correspond to the underlying ridges it passed over, but had an otherwise quite smooth surface (Figure 3.1A). This is in large contrast to the observations of Conway (1897) and Garwood and Gregory (1898), that imaged and described a much more active glacier. Further south, Scott Turnerbreen extended far within the larger extent it had attained by 1936, but its surface was covered in crevasses (Figure 3.1C, G). This most likely signifies the early onset of its surge. Ayerbreen has the most poor coverage of photographs in 1914. It was imaged again in 1920 from an eastern viewpoint, but either the scans or exposures of these photographs yielded blurry results that inhibits a detailed picture. The 1914 photographs nevertheless show a terminus extending to the outer reaches of its terminal moraine, yet the surface was smooth and showed no signs of crevassing. If Ayerbreen surged to its maximal extent, like its geometric changes and forefield geomorphology infer, this must have already happened before 1914. Finally, the glaciers of Foxbreen gave a drastically different impression in 1914 to what they give today (Figures 3.1E, F). Foxbreen dominated the valley bottom, but while displaying a significantly crevassed surface, its terminus was also smoothed by melt. If the glacier had surged, it was likely before this picture was taken.

4.2.3 Geomorphology

Here, the observations are presented which make up the geomorphological maps (Figures 4.6, 4.7). In summary, most landforms found in the forefields of the studied glaciers correspond to polythermal (or previously polythermal) glacier landform assemblages found at other glaciers, for example on Svalbard and in Iceland (Aradóttir et al., 2019; Evans et al., 2012; Schomacker et al., 2014).

Meandering ridges

Meandering ridges with a height of 1–2 m were to a varying extent found in all the studied forefields. They were most abundant at Scott Turnerbreen, where their internal composition was of unconsolidated gravelly sand, overlain by around 30 cm of diamict. They were interpreted to all be supraglacial eskers, due to their composition and that many were clearly traced to active supraglacial meltwater channels.

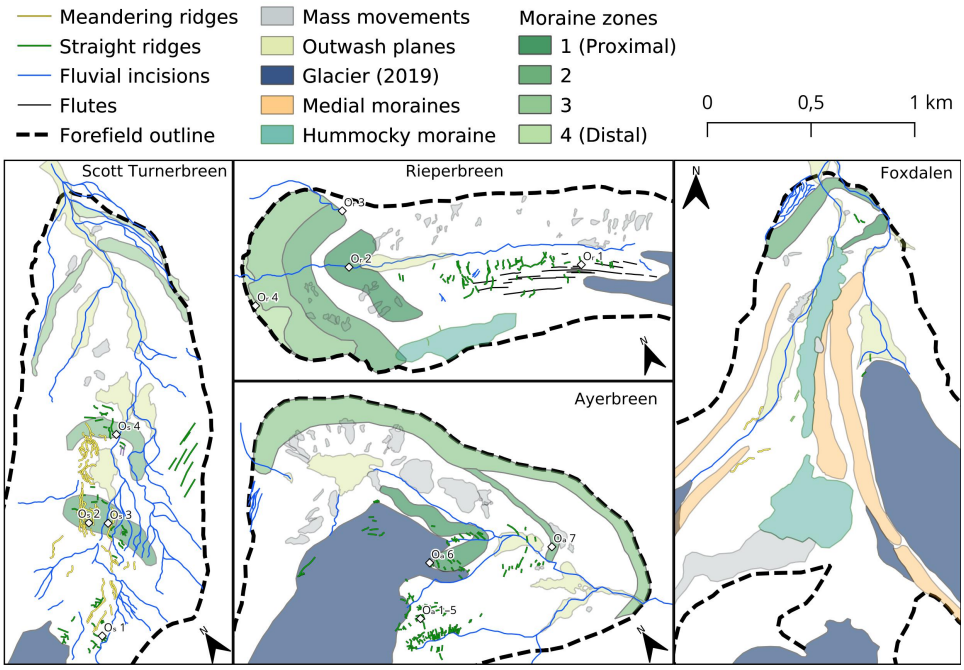

Figure 4.6: Glacier forefield geomorphology. See Table 4.2 for notable field observations (O_x).

Straight ridges

Ridges perpendicular to the past ice flow direction, consisting of diamict with striated clasts with a height of 0.5–2 m, were found in all the studied forefields in Bolterdalen. The detail study near Ayerbreen showed identical ridges melting out of the current glacier surface, which were visibly connected to the glacier bed (Figure 4.7). In each studied case, they were identical in internal composition to the sediment underneath and beside the landforms. These ridges were interpreted as crevasse-squeeze ridges (CSRs), formed during basal infill of crevasses followed by glacier stagnation (Sharp, 1985). The motivation behind this interpretation was from their combinations of perpendicular, oblique and parallel orientations to the past ice flow direction, and the composition of diamict with striated clasts, identical to the underlying and neighbouring sediment composition, indicating that they most likely originated from beneath the glacier. Most notable of these presumed CSRs were indeed those of Ayerbreen, where ridges actively melting out of the glacier could be found along the past glacier centreline under a past glacier thickness of 91 ± 1.3 m in 1936 (Observation O_a6; Figure 4.6, Table 4.2). These ridges were identical in shape and composition to those found at Rieperbreen and Scott Turnerbreen, suggesting that the glaciers had a similar past. Ridges like the presumed CSRs found in Bolterdalen were also identified remotely at the forefield of Foxbreen.

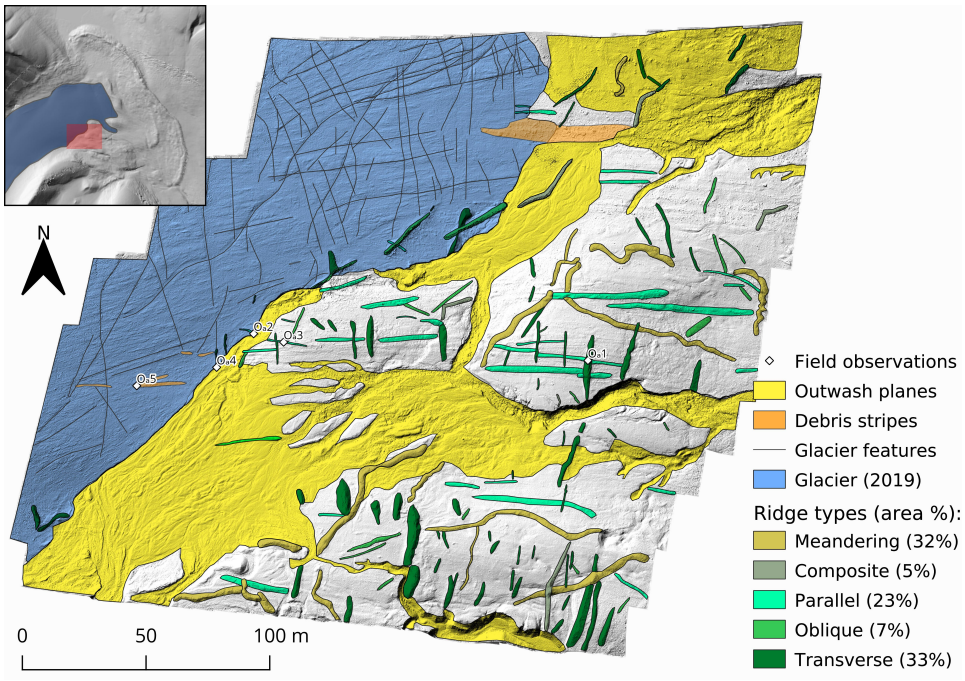

Figure 4.7: Detail study of ridge patterns near Ayerbreen. The distribution of ridges compared to their representative areas is shown in the legend, calculated from the total ridge area (1100 m^2). Field observations from Ayerbreen (O_a) are explained in Table 4.2.

Due to its inaccessibility, however, this was not possible to ground-truth.

Fluvial incisions

Large fluvial activity in the studied forefields is evident through the numerous active and inactive fluvially incisioned channels. The source of water was not always traced to the glaciers, which was most evident at Scott Turnerbreen, indicating that water has also originated from periglacial sources or buried ice. In addition to the dendritic channel networks within the forefields, Scott Turnerbreen, Ayerbreen and Foxbreen also had parallel channels with spacings of 5–20 m along the sides of the forefield edges. These were interpreted to be formed by lateral meltwater channels running along the edges of the past glacier extents or along proglacial snowfields, possibly during their latest advances.

Flutes

Straight 100+ m long ridges, parallel to the past ice flow direction, were abundant in the forefield of Rieperbreen, and similar lineations were seen in every other forefield. At Rieperbreen, these consisted of diamict with striated clasts, and were interpreted as flutes, found when a polythermal glacier preserves its subglacial landforms if its terminus is cold-based during retreat (Eklund and Hart, 1996).

Mass movements and hummocky moraine

Buried glacier ice was an abundant occurrence in all of the studied forefields. Signs of mass movements, were clustered and always revealed buried ice when observed up close, under about 1 m of diamict. Certain areas in the forefields of Rieperbreen and the Foxdalen glacier complex also had a much more uneven and hummocky expression than neighbouring areas, and these were assumed to contain glacier ice that has not yet been exposed. Such considerable thicknesses of sediment overlaying ice can be produced both by sub- to englacial thrusting or by multiple glacier advances overriding older ice (Everest and Bradwell, 2003; Ham and Attig, 2008; Hambrey et al., 1996). This abundance of ice is therefore urged to study further, to shed further light on the past dynamics of the respective glaciers.

Outwash planes

Individual outwash planes of up to 40 000 m^2 were mapped in the studied forefields. They correspond to gentle slopes in the landscape, which are common in the study area due to the horizontal geological sedimentary sequences. These areas of fluvial erosion and deposition have erased many previous landforms, exemplified by Rieperbreen having a complex of ridges near its terminus in 1961, where there is only an outwash plane today.

Medial moraines

The glaciers of Foxdalen have created large 10–30 m high and up to 2 km long medial moraines between their historic boundaries. Glacier ice with clear structural deformation were observed in them, supporting the interpretation that they are mainly composed of ice that has had a more dynamic past than today.

Moraine zones

The most prominent outer moraines in all the studied glacier forefields are today 15–50 m high and 70–120 m wide. All of them showed signs of either exposed glacier ice, abundant mass movements, a hummocky surface expression, or a combination of the three, indicating that they are all most likely ice-cored. The age of the outermost moraines in the studied forefields could put in context in relation to the 1914 photographs. At Rieperbreen, the glacier seemed to have reached its approximate outermost geomorphologically visible extent in 1914, but a sharp boundary in lichen cover suggests that the outermost tens of metres may be a composite of something older. Scott Turnerbreen reached its largest extent sometime between 1936 and 1961, but older moraines seem to exist farther out which indicates that its mid-1900s extent was not the largest during the late Holocene. Ayerbreen and Foxbreen, however, seem to have reached their maximum late Holocene extents near 1914 as no signs were found of more distal moraines. Since Foxbreen advanced in front of Fleinisen, no distal landforms seem to have been preserved there either.

In addition to the previously mentioned moraines, multiple larger lobe-formed ridges, transverse to the past ice-flow direction consisting of diamict with striated clasts, were found in the forefields of Rieperbreen, Scott Turnerbreen and Ayerbreen. These were 25–150 m wide in the short axis, and 400–800 m wide, with heights of 10–30 m. They indicate a net depositional environment, along arches that resemble reasonable terminus positions, and were therefore interpreted as overridden front moraines. Due to their considerable sediment thicknesses, they probably formed in a different manner than ice-cored moraines such as those left behind by the latest advance of Scott Turnerbreen, explained in detail by Sletten et al. (2008), and by the Foxdalen glacier complex. Historic imagery of these glaciers show bands of crevasses above the presently exposed ridges (Figures 3.1A, C, G), proving that they are indeed older than the latest advance.

Table 4.2: Field observations. See Figure 4.6 and 4.7 for their respective locations.

	Ayerbreen
O_a1	L-shaped ridge composed by diamict with striated clasts. Shale is the dominant lithology.
O_a2	Ridge parallel to ice-flow direction, vertically melting out of the ice and reaching the glacier bed.
O_a3	Proglacial continuation of ridge at O_a2.
O_a4	Ridge transversal to ice-flow direction, vertically melting out of the ice and reaching the glacier bed.
O_a5	Englacially sourced debris, predominantly consisting of sandstone.
O_a6	Transverse ridge like O_a4, but over 2 m high and with >1 m wide striated clasts.
O_a7	Large ridge consisting of at least 5 m of diamict with striated clasts.
	Scott Turnerbreen
O_s1	Ridge transverse to ice-flow of diamict with striated clasts, compositionally similar to the substrate.
O_s2	Meandering ridge consisting of gravelly sand, overlain by 30 cm of diamict.
O_s3	Forefield-wide ridge, consisting of ~10 m of diamict over bedrock exposures.
O_s4	Lobe-shaped forefield-wide ridge, consisting of at least 7 m of diamict. No bedrock was seen.
	Rieperbreen
O_r1	Ridge transverse to ice-flow direction consisting of diamict with striated clasts.
O_r2	Lobe-shaped ridge with an exposed sediment thickness of ~13 m, consisting of diamict.
O_r3	Folded and tectonised glacier ice outcrop, overlain by 1m of striated diamict.
O_r4	Moraine crest overlaying an old glacifluvial channel.

5

Discussion

Geodetic, observational and geomorphological inferences indicate that four out of the five studied glaciers seemed to have surged within a few decades of each other (Figure 4.1). Coupled with the high frequency of Svalbard-wide observations and inferences by Farnsworth et al. (2016), it is likely that this event was widespread throughout the archipelago. Other studies have noted the peculiar phenomenon of surges having been more frequently observed near the end of the LIA (e.g. Dowdeswell et al., 1995; Nuth et al., 2019; Sevestre et al., 2015). Furthermore, Sevestre et al. (2015) suggested that the specific climate of Svalbard during the LIA may have been optimal for surging to occur. This must bear truth, as the climate of Svalbard is near the centre of the highest surge frequency (Figure 1.1). But a fact that has so far been given inadequate emphasis is that observations of early explorers do not represent the LIA as a whole; they represent the near-end of the LIA. The over-400 forefields with CSRs identified by Farnsworth et al. (2016) indicate that the largest LIA extent of most glaciers were attained by surging, which occurred at the same time as large step-like increases in temperature (Humlum et al., 2005; Nordli et al., 2014). Therefore, not just the climate, but its *changes* might be essential for understanding why many glaciers would surge within such a short time-period.

The surge of Scott Turnerbreen is of special interest, as its active phase at a first glance seems to have lasted for multiple decades. This is exceptionally long for a surge on Svalbard, so another alternate explanation is dividing the activity of Scott Turnerbreen into two separate events; a normal surge, followed by an

abnormal continued advance. In 1914, the glacier surface was entirely covered by crevasses, indicating a highly active state (Figures 3.1C, G). In the 1936 photographs extensive crevassing was not apparent any more, yet it continued advancing until sometime before 1961. Maybe the surge did not last for this entire period, but the ~1914 surge displaced so much mass that the glacier could uphold a high-energy flow even long afterwards. Glacier surges on Svalbard often terminate in near-total stagnation and trend toward a cold basal regime at the tongue or throughout the glacier (e.g. Melvold and Hagen, 1998; Nuttall et al., 1997; Sevestre et al., 2015). Total stagnation has undoubtedly happened at Scott Turnerbreen by now, earliest shown by Hodgkins et al. (1999), but unlike other glaciers, its surge seems to have ended not directly in stagnation but in a continued period of high activity. This *post-surge advance* has not yet been described at other glaciers, but due to the sparsity of observational data on Svalbard, it may still have happened elsewhere. The implications of such a phenomenon could be significant, as Scott Turnerbreen essentially lost all of its potential of longevity by wasting its mass through surging.

An active question is whether glaciers can acquire a surge type behaviour due to changes in climate, but also whether glaciers with a history of surging will do so in the future as well. Out of the four studied glaciers that are believed to have surged, they all lost between 73% and 91% of their volumes in 1936–2019. This melt has consequently made them up to 26% steeper (Figure 4.4, Table 4.1), which theoretically increases their chances for fast flow, and thus their chances to surge (Benn et al., 2019a). A similar phenomenon is common on tidewater glaciers, where a steepening due to melt has been shown to induce surges initiated at the terminus (Sevestre et al., 2018). In the case of the small terrestrial glaciers in Bolterdalen and Foxdalen, however, this steepening was concurrent with excessive volume loss, and the critical pressures needed to surge are therefore now much harder to reach. But this does not mean that small glaciers cannot surge, exemplified by a 2 km long glacier and its 1.7 km long neighbour, about 10 km east of the study area, that surged at the same time when they were surveyed by the NPI in 2009 ($78.08°N$, $16.63°E$; www.toposvalbard.npolar.no). The glaciers that were presumed to surge in the study area have subsequently shown positive thickness change in their accumulation areas, further leaning toward the potential of future surging (Figure 4.3). This is however a reducing trend, and the only glaciers with thickness gains above 0.4 m/a in 2009–2019 were Ayerbreen and Foxbreen. While spotty thickness gains and increasingly steep surfaces are indicative that they may surge in the future, these phenomena might be compensated by further warming, thus hindering further build-up of mass which would be needed to surge again.

The abundance of overridden sediment deposits at Rieperbreen, Scott Turnerbreen and Ayerbreen, hereby assumed to be moraines, may tell a story about their

history before the observational period. Moraines are generally assumed to be preserved poorly when overridden by a temperate glacier (Hallet et al., 2013). Thus, the presence of overridden moraines either indicate that the overriding glaciers were cold-based, which was obviously not the case here, or that strong subglacial erosion only occurred within a short time span. Old landforms have been shown to survive fast-lived surges (Flink et al., 2015, 2018; Ottesen and Dowdeswell, 2006), and the presence of preserved overridden moraines are therefore further indicators of surging instead of normal glacier activity. Furthermore, since the overridden moraines were up to (at least) 13 m thick and showed no signs of internal structure nor buried ice, their formation probably indicates previous stable or near-stable glacier configurations, since it indicates decadal or centennial rather than annual build-up. Care should however be taken in this assumption before further studies can show whether they are indeed are mainly composed of sediment or rather of ice, since the exposed outcrops are not guaranteed to be representative for the entire landform. Furthermore, no one has noted the abundance of overridden moraine candidates in central Svalbard before, e.g. at Aldegondabreen, Renardbreen, Methuenbreen, Richterbreen, Tellbreen and many others (see www.toposvalbard.npolar.no). The internal composition needs to be examined to be certain about these cases, but based on the observations of this study, it may indicate that one or many previous stable regional glacier configurations have been preserved in spite of larger subsequent advances. It fits well into the earlier conclusion that many or most late-LIA extents were probably reached by means of surging, since the preserved moraines could suggestively indicate stable positions before their final advance. Digging into more of these ridges is one way to strengthen or weaken our view on the interplay of climate change and glacier surges, and is urged to study further.

The results of this study suggests that sudden warming may be able to trigger widespread surging, but one major question remains; how would this happen? Benn et al. (2019a) indicated that the main trigger for surging is through large enthalpy inputs to the glacier bed, and that the main process for this is through meltwater reaching the glacier bed through crevasses. This leads to a runaway enthalpy production, with further crevassing and thus increasing enthalpy input. Their enthalpy equation is almost identical to that of Wilson and Flowers (2013) who evaluated the environmental controls of a glacier's thermal regime. The equations from the two studies however differ by having two completely different main enthalpy sources; the first is through crevassing, and the latter is through latent heat production by perennial near-surface firn aquifers. This dichotomy yields potential that more enthalpy sources than just crevassing could be incorporated into the model by Benn et al. (2019a) to trigger a glacier to surge. Perennial firn aquifers exist within certain combinations of snow melt and accumulation, where too little melt leads to the meltwater

freezing during the winter, but too much of it will thin the firn thickness so it can no longer insulate liquid water during the winter (van Pelt et al., 2016). Based on this, interesting scenarios are possible when rapid climate change is considered. On Svalbard, the LIA seemed to be much colder than what was seen since the 1900s, and cold-based glaciers are believed to have been the norm (Sevestre et al., 2015). Today, previously dry accumulation zones are in the process developing firn aquifers (Marchenko, 2018; van Pelt et al., 2016). This evolution requires a thick enough firn layer to house the water, so it has not been observed on smaller glaciers. With Svalbard's transition from cold to warmer temperatures, however, firn thicknesses on smaller glaciers in the past may have been considerably larger. For a few tens of years with high melt and abundant firn, perennial firn aquifers may therefore have temporarily existed, before excessive melt led to the firn thicknesses seen today of often less than 3 m (Jaedicke and Sandvik, 2002; van Pelt et al., 2019). The importance of perennial firn aquifers as enthalpy sources, contrasted with the consequences of similar sources, shows that changes in firn properties during climate change may affect a glacier's potential to surge, and is therefore a possible explanation for why glaciers seemed to surge near the same time near the end of the LIA.

6

Conclusion

The aim of this study was to investigate the reason behind the confusion around when, how and why most glaciers reached their maximum LIA extents in an explosive manner. Already published evidence suggests that a majority of these advances may have been reached by means of surging, which implies that surges may occur as a response to rapid climate change. It may mean that future warming could trigger widespread surging, maybe explaining the recently observed surge at Severnaya Zemlya (Willis et al., 2018). This phenomenon was further examined by building on the work of Sevestre and Benn (2015), by identifying both the climatic envelope of areas where surges have been recorded, and additionally which areas have a climatic trend toward it. The resultant empirical forecasting suggests that other Arctic, Himalayan and Antarctic regions trend toward the specific climate seen on Svalbard, and we may for that reason see more surges there in the future. In Bolterdalen and Foxdalen on Svalbard, the histories of five glaciers were studied in depth to shed light on why four of them seemed to have surged within just a few decades of each other. This was done using aerial image and drone photogrammetric surveying, geomorphological mapping, and interpretation of historic observations. Results showed an average glacier volume loss of 81% ± 7%, and a halving in areal extent between 1936 and 2019. In addition, Scott Turnerbreen may have experienced unprecedented mass wastage by upholding a high-energy flow type for somewhere between 22 and 47 years after its surge around 1914. During 1936–2019, the glacier consequently lost 91% ± 5% of its volume, which is 24% more than the other four glaciers on average, and this phenomenon should be looked for elsewhere to evaluate how

common it is. The question of how surges can be triggered by rapid warming events is still not answered, but a suggested mechanism is that saturation of the firn zone by suddenly increasing melt may provide a spike in enthalpy input through latent heat release, possibly high enough to trigger a surge. The questions raised in the study show that further research in the subject is integral, as we may see major ice mass collapses in the future if global warming follows its current trajectory, a phenomenon that may need to be accounted for in future ice loss projections.

Bibliography

Agassiz L. 1838. On the polished and striated surfaces of the rocks which form the beds of glaciers in the Alps. Proc. Geol. Soc. London 3:321–322.

Ahlmann HW. 1953. Glacier variations and climatic fluctuations. Technical report. American Geographical Society. Series: Bowman Memorial Lectures. Ser. III. The American Geographical Society.

Aradóttir N, Ingólfsson Ó, Noormets R, Benediktsson ÍÖ, Ben-Yehoshua D, Håkansson L, Schomacker A. 2019. Glacial geomorphology of Trygghamna, western Svalbard - Integrating terrestrial and submarine archives for a better understanding of past glacial dynamics. Geomorphology 344:75–89. doi:10.1016/j.geomorph.2019.07.007.

Aschwanden A, Bueler E, Khroulev C, Blatter H. 2012. An enthalpy formulation for glaciers and ice sheets. Journal of Glaciology 58:441–457. doi:10.3189/2012JoG11J088.

Bælum K, Benn DI. 2011. Thermal structure and drainage system of a small valley glacier (Tellbreen, Svalbard), investigated by ground penetrating radar. The Cryosphere 5:139–149. doi:10.5194/tc-5-139-2011.

Barr S. 2009. Gunnar Isachsen. Norsk biografisk leksikon .

Benn DI, Fowler AC, Hewitt I, Sevestre H. 2019a. A general theory of glacier surges. Journal of Glaciology 65:701–716. doi:10.1017/jog.2019.62.

Benn DI, Jones RL, Luckman A, Fürst JJ, Hewitt I, Sommer C. 2019b. Mass and enthalpy budget evolution during the surge of a polythermal glacier: a test of theory. Journal of Glaciology 65:717–731. doi:10.1017/jog.2019.63.

Björnsson H. 1981. Radio-Echo Sounding Maps of Storglaciären, Isfallsglaciären and Rabots Glaciär, Northern Sweden. Geografiska Annaler. Series A, Physical Geography 63:225. doi:10.2307/520835.

Björnsson H, Gjessing Y, Hamran SE, Hagen JO, Liestøl O, Pálsson F, Erlingsson B. 1996. The thermal regime of sub-polar glaciers mapped by multi-frequency radio-echo sounding. Journal of Glaciology 42:23–32. doi: 10.3189/S0022143000030495.

Boulton GS, Paul MA. 1976. The influence of genetic processes on some geotechnical properties of glacial tills. Quarterly Journal of Engineering Geology and Hydrogeology 9:159–194. doi:10.1144/GSL.QJEG.1976.009.03.03.

Bull C, Carnein CR. 1970. The mass balance of a cold glacier: Meserve Glacier, south Victoria Land, Antarctica. Ohio State University, Institute of Polar Sciences .

Christiansen HH, Humlum O, Eckerstorfer M. 2013. Central Svalbard 2000–2011 Meteorological Dynamics and Periglacial Landscape Response. Arctic, Antarctic, and Alpine Research 45:6–18. doi:10.1657/1938-4246-45.16.

Conway WM. 1897. The First Crossing of Spitsbergen. London : J.M. Dent & Co. ; New York : C. Scribner's Sons.

Copernicus Climate Change Service. 2019. ERA5 monthly averaged data on single levels from 1979 to present. ECMWF. doi:10.24381/CDS.F17050D7.

Copland L, Sylvestre T, Bishop MP, Shroder JF, Seong YB, Owen LA, Bush A, Kamp U. 2011. Expanded and Recently Increased Glacier Surging in the Karakoram. Arctic, Antarctic, and Alpine Research 43:503–516. doi: 10.1657/1938-4246-43.4.503.

Dallmann WK. 2007. Geology of Svalbard. Geology of the land and sea areas of northern Europe. Norges Geologiske Undersøkelse Special Publication 10:87–89.

D'Andrea WJ, Vaillencourt DA, Balascio NL, Werner A, Roof SR, Retelle M, Bradley RS. 2012. Mild Little Ice Age and unprecedented recent warmth in an 1800 year lake sediment record from Svalbard. Geology 40:1007–1010. doi:10.1130/G33365.1.

De Geer G. 1910. Guide de l'excursion au Spitsberg: Excursion A1 (Guide to excursions on Spitsbergen: Excursion A1), paper presented at XI International Geological Congress. Exec. Comm., Stockholm .

Divine D, Isaksson E, Martma T, Meijer HA, Moore J, Pohjola V, van de Wal RSW, Godtliebsen F. 2011. Thousand years of winter surface air temperature

variations in Svalbard and northern Norway reconstructed from ice-core data. Polar Research 30:7379. doi:10.3402/polar.v30i0.7379.

Divine DV, Dick C. 2006. Historical variability of sea ice edge position in the Nordic Seas. Journal of Geophysical Research 111:C01001. doi:10.1029/2004JC002851.

Dowdeswell JA, Drewry DJ, Liestøl O, Orheim O. 1984. Airborne radio echo sounding of sub-polar glaciers in Spitsbergen. volume 182. Oslo: Norsk Polarinstitutt Skrifter.

Dowdeswell JA, Hamilton GS, Hagen JO. 1991. The duration of the active phase on surge-type glaciers: contrasts between Svalbard and other regions. Journal of Glaciology 37:388–400. doi:10.3189/S0022143000005827.

Dowdeswell JA, Hodgkins R, Nuttall AM, Hagen JO, Hamilton GS. 1995. Mass balance change as a control on the frequency and occurrence of glacier surges in Svalbard, Norwegian High Arctic. Geophysical Research Letters 22:2909–2912. doi:10.1029/95GL02821.

Dujardin JR, Bano M. 2013. Topographic migration of GPR data: Examples from Chad and Mongolia. Comptes Rendus Geoscience 345:73–80. doi:10.1016/j.crte.2013.01.003.

Dunse T, Schellenberger T, Hagen JO, Kääb A, Schuler TV, Reijmer CH. 2015. Glacier-surge mechanisms promoted by a hydro-thermodynamic feedback to summer melt. The Cryosphere 9:197–215. doi:10.5194/tc-9-197-2015.

Eisen O, Harrison WD, Raymond CF. 2001. The surges of Variegated Glacier, Alaska, U.S.A., and their connection to climate and mass balance. Journal of Glaciology 47:351–358. doi:10.3189/172756501781832179.

Eklund A, Hart JK. 1996. Glaciotectonic deformation within a flute from the Isfallsglaciären, Sweden. Journal of Quaternary Science 11:299–310. doi:10.1002/(SICI)1099-1417(199607/08)11:4<299::AID-JQS255>3.0.CO;2-C. _eprint: https://onlinelibrary.wiley.com/doi/pdf/10.1002/%28SICI%291099-1417%28199607/08%2911%3A4%3C299%3A%3AAID-JQS255%3E3.0.CO%3B2-C.

Evans DJ, Storrar RD, Rea BR. 2016. Crevasse-squeeze ridge corridors: Diagnostic features of late-stage palaeo-ice stream activity. Geomorphology 258:40–50. doi:10.1016/j.geomorph.2016.01.017.

Evans DJ, Strzelecki M, Milledge DG, Orton C. 2012. Hørbyebreen polythermal

glacial landsystem, Svalbard. Journal of Maps 8:146–156. doi:10.1080/17445647.2012.680776.

Everest J, Bradwell T. 2003. Buried glacier ice in southern Iceland and its wider significance. Geomorphology 52:347–358. doi:10.1016/S0169-555X(02)00277-5.

Farnsworth WR, Ingólfsson Ó, Noormets R, Allaart L, Alexanderson H, Henriksen M, Schomacker A. 2017. Dynamic Holocene glacial history of St. Jonsfjorden, Svalbard. Boreas 46:585–603. doi:10.1111/bor.12269.

Farnsworth WR, Ingólfsson Ó, Retelle M, Allaart L, Håkansson LM, Schomacker A. 2018. Svalbard glaciers re-advanced during the Pleistocene-Holocene transition. Boreas 47:1022–1032. doi:10.1111/bor.12326.

Farnsworth WR, Ingólfsson Ó, Retelle M, Schomacker A. 2016. Over 400 previously undocumented Svalbard surge-type glaciers identified. Geomorphology 264:52–60. doi:10.1016/j.geomorph.2016.03.025.

Flink AE, Hill P, Noormets R, Kirchner N. 2018. Holocene glacial evolution of Mohnbukta in eastern Spitsbergen. Boreas 47:390–409. doi:10.1111/bor.12277.

Flink AE, Noormets R, Kirchner N, Benn DI, Luckman A, Lovell H. 2015. The evolution of a submarine landform record following recent and multiple surges of Tunabreen glacier, Svalbard. Quaternary Science Reviews 108:37–50. doi:10.1016/j.quascirev.2014.11.006.

Flint RF, Sanders JE, Rodgers J. 1960. DIAMICTITE, A SUBSTITUTE TERM FOR SYMMICTITE. Geological Society of America Bulletin 71:1809. doi:10.1130/0016-7606(1960)71[1809:DASTFS]2.0.CO;2.

Forster RR, Box JE, van den Broeke MR, Miège C, Burgess EW, van Angelen JH, Lenaerts JTM, Koenig LS, Paden J, Lewis C, Gogineni SP, Leuschen C, McConnell JR. 2014. Extensive liquid meltwater storage in firn within the Greenland ice sheet. Nature Geoscience 7:95–98. doi:10.1038/ngeo2043.

Fürst JJ, Gillet-Chaulet F, Benham TJ, Dowdeswell JA, Grabiec M, Navarro F, Pettersson R, Moholdt G, Nuth C, Sass B, Aas K, Fettweis X, Lang C, Seehaus T, Braun M. 2017. Application of a two-step approach for mapping ice thickness to various glacier types on Svalbard. The Cryosphere 11:2003–2032. doi:10.5194/tc-11-2003-2017.

Fürst JJ, Navarro F, Gillet-Chaulet F, Huss M, Moholdt G, Fettweis X, Lang C,

Seehaus T, Ai S, Benham TJ, Benn DI, Björnsson H, Dowdeswell JA, Grabiec M, Kohler J, Lavrentiev I, Lindbäck K, Melvold K, Pettersson R, Rippin D, Saintenoy A, Sánchez-Gámez P, Schuler TV, Sevestre H, Vasilenko E, Braun MH. 2018. The Ice-Free Topography of Svalbard. Geophysical Research Letters 45:11,760–11,769. doi:10.1029/2018GL079734.

Garwood EJ, Gregory JW. 1898. Contributions to the Glacial Geology of Spitsbergen. Quarterly Journal of the Geological Society 54:197–227. doi:10.1144/GSL.JGS.1898.054.01-04.18.

Geikie A. 1863. On the phenomena of the glacial drift of Scotland. volume 1. Published for the Society of J. Gray.

Girod L, Nielsen NI, Couderette F, Nuth C, Kääb A. 2018. Precise DEM extraction from Svalbard using 1936 high oblique imagery. Geoscientific Instrumentation, Methods and Data Systems 7:277–288. doi:10.5194/gi-7-277-2018.

Gregory JW, Garwood M, Trevor-Battye M. 1897. The First Crossing of Spitsbergen: Discussion. The Geographical Journal 9:365–368. Publisher: [Wiley, Royal Geographical Society (with the Institute of British Geographers)].

Hagen JO, Liestøl O, Roland E, Jørgensen T, editors. 1993. Glacier atlas of Svalbard and Jan Mayen. Number 129 in Meddelelser / Norsk Polarinstitutt. Oslo: Nork Polarinstitutt. OCLC: 612170272.

Hallet B, Hunter L, Bogen J. 2013. Rates of erosion and sediment evacuation by glaciers. Fluv Geom: Geom Crit Conc Vol 12:213–35. Publisher: Routledge.

Ham NR, Attig JW. 2008. Ice wastage and landscape evolution along the southern margin of the Laurentide Ice Sheet, north-central Wisconsin. Boreas 25:171–186. doi:10.1111/j.1502-3885.1996.tb00846.x.

Hamberg A. 1894. En resa till norra Ishafvet sommaren 1892. Ymer 14:25–61.

Hambrey MJ. 2005. Structure and changing dynamics of a polythermal valley glacier on a centennial timescale: Midre Lovénbreen, Svalbard. Journal of Geophysical Research 110. doi:10.1029/2004JF000128.

Hambrey MJ, Dowdeswell JA, Murray T, Porter PR. 1996. Thrusting and debris entrainment in a surging glacier: Bakaninbreen, Svalbard. Annals of Glaciology 22:241–248. doi:10.3189/1996AoG22-1-241-248.

Hansen S. 2003. From surge-type to non-surge-type glacier behaviour: midre Lovénbreen, Svalbard. Annals of Glaciology 36:97–102. doi: 10.3189/172756403781816383.

Hanssen-Bauer I, Førland EJ, Hisdal H, Mayer S, Sandø AB, Sorteberg A, Adakudlu M, Andresen J, Bakke J, Beldring S, Benestad R, Bilt W, Bogen J, Borstad C, Breili K, Breivik Ø, Børsheim KY, Christiansen HH, Dobler A, Engeset R, Frauenfelder R, Gerland S, Gjelten HM, Gundersen J, Isaksen K, Jaedicke C, Kierulf H, Kohler J, Li H, Lutz J, Melvold K, Mezghani A, Nilsen F, Nilsen IB, Nilsen JEØ, Pavlova O, Ravndal O, Risebrobakken B, Saloranta T, Sandven S, Schuler TV, Simpson MJR, Skogen M, Smedsrud LH, Sund M, Vikhamar-Schuler D, Westermann S, Wong WK. 2019. Climate in Svalbard 2100. Technical Report M-1242. Norwegian Environment Agency. doi:10.13140/RG.2.2.10183.75687.

Hock R. 2003. Temperature index melt modelling in mountain areas. Journal of Hydrology 282:104–115. doi:10.1016/S0022-1694(03)00257-9.

Hodgkins R, Hagen JO, Hamran SE. 1999. 20th century mass balance and thermal regime change at Scott Turnerbreen, Svalbard. Annals of Glaciology 28:216–220. doi:10.3189/172756499781821986.

Holmlund ES. in review. Near constant glacier melt over 106 years revealed using structure-from-motion photogrammetry on untapped archival resource — Aldegondabreen, Svalbard. Journal of Glaciology -.

Holmlund ES, Holmlund P. 2019. Constraining 135 Years of Mass Balance with Historic Structure-from-Motion Photogrammetry on Storglaciären, Sweden. Geografiska Annaler: Series A, Physical Geography doi:10.1080/04353676.2019.1588543.

Holmlund P, Martinsson T. 2016. Frusna ögonblick: svensk polarfotografi 1861-1980. Stockholm: Art and Theory Publishing.

Hong SH, Jung HS, Won JS. 2006. Extraction of ground control points (GCPs) from synthetic aperture radar images and SRTM DEM. International Journal of Remote Sensing 27:3813–3829. doi:10.1080/01431160600658115.

Hormes A, Gjermundsen EF, Rasmussen TL. 2013. From mountain top to the deep sea – Deglaciation in 4D of the northwestern Barents Sea ice sheet. Quaternary Science Reviews 75:78–99. doi:10.1016/j.quascirev.2013.04.009.

Huber E, Hans G. 2018. RGPR — An open-source package to process and visualize GPR data. In: 2018 17th International Conference on Ground

Penetrating Radar (GPR). Rapperswil, Switzerland: IEEE. p. 1–4. doi:10.1109/ICGPR.2018.8441658.

Hughes ALC, Gyllencreutz R, Lohne ØS, Mangerud J, Svendsen JI. 2016. The last Eurasian ice sheets - a chronological database and time-slice reconstruction, DATED-1. Boreas 45:1–45. doi:10.1111/bor.12142.

Humlum O. 2002. Modelling late 20th-century precipitation in Nordenskiold Land, Svalbard, by geomorphic means. Norsk Geografisk Tidsskrift - Norwegian Journal of Geography 56:96–103. doi:10.1080/00291950276005641 3.

Humlum O, Elberling B, Hormes A, Fjordheim K, Hansen OH, Heinemeier J. 2005. Late-Holocene glacier growth in Svalbard, documented by subglacial relict vegetation and living soil microbes. The Holocene 15:396–407. doi:10.1191/0959683605hl817rp.

Isachsen G. 1912. Exploration du Nord-Ouest du Spitsberg entreprise sous les auspices de S.A.S. le Prince de Monaco par la Mission Isachsen. Premiére Partie Résultats des Campagnes Scientifiques Accomplies sur son Yacht par Albert ler, Prince Souverain de Monaco 40.

ISO 14688-1. 2002. Geotechnical investigation and testing — Identification and classification of soil — Part 1: Identification and description. Standard. International Organization for Standardization. Geneva, CH.

Jaedicke C, Sandvik AD. 2002. High resolution snow distribution data from complex Arctic terrain: a tool for model validation. Natural Hazards and Earth System Science 2:147–155. Publisher: Copernicus Publications on behalf of the European Geosciences Union.

Jamieson SSR, Ewertowski MW, Evans DJA. 2015. Rapid advance of two mountain glaciers in response to mine-related debris loading: Mine Waste and Glacier Advance. Journal of Geophysical Research: Earth Surface 120:1418–1435. doi:10.1002/2015JF003504.

Jiskoot H, Murray T, Boyle P. 2000. Controls on the distribution of surge-type glaciers in Svalbard. Journal of Glaciology 46:412–422. doi:10.3189/172756500781833115.

Jiskoot H, Murray T, Luckman A. 2003. Surge potential and drainage-basin characteristics in East Greenland. Annals of Glaciology 36:142–148. doi:10.3189/172756403781816220.

Karlén W. 1973. Holocene Glacier and Climatic Variations, Kebnekaise Mountains, Swedish Lapland. Geografiska Annaler. Series A, Physical Geography 55:29. doi:10.2307/520485.

Kjær KH, Korsgaard NJ, Schomacker A. 2008. Impact of multiple glacier surges—a geomorphological map from Brúarjökull, East Iceland. Journal of Maps 4:5–20. doi:10.4113/jom.2008.91.

Larsen E, Lysså A, Rubensdotter L, Farnsworth WR, Jensen M, Nadeau MJ, Ottesen D. 2018. Lateglacial and Holocene glacier activity in the Van Mijenfjorden area, western Svalbard. arktos 4. doi:10.1007/s41063-018-0042-2.

Lefauconnier B, Hagen JO. 1991. Surging and calving glaciers in eastern Svalbard. Number 116 in Meddelelser / Norsk Polarinstitutt. Oslo: Norsk Polarinst. OCLC: 221356160.

Liestøl O. 1969. Glacier surges in West Spitsbergen. Canadian Journal of Earth Sciences 6:895–897. doi:10.1139/e69-092.

Liestøl O. 1988. The glaciers in the Kongsfjorden area, Spitsbergen. Norsk Geografisk Tidsskrift - Norwegian Journal of Geography 42:231–238. doi:10.1080/00291958808552205.

Lingle CS, Brown TJ. 1987. A Subglacial Aquifer Bed Model and Water Pressure Dependent Basal Sliding Relationship for a West Antarctic Ice Stream. In: CJ Van der Veen, J Oerlemans, editors. Dynamics of the West Antarctic Ice Sheet. Dordrecht: Springer Netherlands. p. 249–285.

Lovell H, Benn DI, Lukas S, Ottesen D, Luckman A, Hardiman M, Barr ID, Boston CM, Sevestre H. 2018. Multiple Late Holocene surges of a High-Arctic tidewater glacier system in Svalbard. Quaternary Science Reviews 201:162–185. doi:10.1016/j.quascirev.2018.10.024.

Lysså A, Lønne I. 2001. Moraine development at a small High-Arctic valley glacier: Rieperbreen, Svalbard: MORAINE DEVELOPMENT IN SVALBARD. Journal of Quaternary Science 16:519–529. doi:10.1002/jqs.613.

Mangerud J, Landvik JY. 2007. Younger Dryas cirque glaciers in western Spitsbergen: smaller than during the Little Ice Age. Boreas 36:278–285. doi:10.1080/03009480601134827.

Marchenko S. 2018. Subsurface fluxes of mass and energy at the accumulation zone of Lomonosovfonna ice cap, Svalbard. Uppsala University. PhD Thesis.

Martín-Moreno R, Allende Álvarez F, Hagen JO. 2017. 'Little Ice Age' glacier extent and subsequent retreat in Svalbard archipelago. The Holocene 27:1379–1390. doi:10.1177/0959683617693904.

Meier MF, Post A. 1969. What are glacier surges? Canadian Journal of Earth Sciences 6:807–817. doi:10.1139/e69-081.

Meier MF, Post A. 1987. Fast tidewater glaciers. Journal of Geophysical Research 92:9051. doi:10.1029/JB092iB09p09051.

Melvold K, Hagen JO. 1998. Evolution of a Surge-Type Glacier in its Quiescent Phase: Kongsvegen, Spitsbergen, 1964–95. Journal of Glaciology 44:394–404. doi:10.3189/S0022143000002720.

Mertes JR, Gulley JD, Benn DI, Thompson SS, Nicholson LI. 2017. Using structure-from-motion to create glacier DEMs and orthoimagery from historical terrestrial and oblique aerial imagery: SfM on Differing Historical Glacier Imagery Sets. Earth Surface Processes and Landforms 42:2350–2364. doi:10.1002/esp.4188.

Miller GH, Landvik JY, Lehman SJ, Southon JR. 2017. Episodic Neoglacial snowline descent and glacier expansion on Svalbard reconstructed from the 14C ages of ice-entombed plants. Quaternary Science Reviews 155:67–78. doi:10.1016/j.quascirev.2016.10.023.

Mölg T, Cullen NJ, Hardy DR, Kaser G, Klok L. 2008. Mass balance of a slope glacier on Kilimanjaro and its sensitivity to climate. International Journal of Climatology 28:881–892. doi:10.1002/joc.1589.

Mouginot J, Bjørk AA, Millan R, Scheuchl B, Rignot E. 2018. Insights on the Surge Behavior of Storstrømmen and L. Bistrup Bræ, Northeast Greenland, Over the Last Century. Geophysical Research Letters 45. doi: 10.1029/2018GL079052.

Murray T, Luckman A, Strozzi T, Nuttall AM. 2003. The initiation of glacier surging at Fridtjovbreen, Svalbard. Annals of Glaciology 36:110–116. doi: 10.3189/172756403781816275.

Nathorst AG. 1900. Två somrar i Norra Ishafvet. volume 1. Stockholm: Beijers Bokförlagsaktiebolag.

Nordli Ø, Przybylak R, Ogilvie AE, Isaksen K. 2014. Long-term temperature trends and variability on Spitsbergen: the extended Svalbard Airport temperature series, 1898–2012. Polar Research 33:21349. doi:10.3402/polar.

v33.21349.

Norwegian Polar Institute. 2014. Terrengmodell Svalbard (So Terrengmodell). doi:10.21334/npolar.2014.dce53a47. Type: dataset.

Norwegian Polar Institute. 2016. Geological map of Svalbard (1:250000). doi:10.21334/NPOLAR.2016.616F7504. Type: dataset.

Nuth C, Gilbert A, Köhler A, McNabb R, Schellenberger T, Sevestre H, Weidle C, Girod L, Luckman A, Kääb A. 2019. Dynamic vulnerability revealed in the collapse of an Arctic tidewater glacier. Scientific Reports 9. doi:10.1038/s41598-019-41117-0.

Nuth C, Kohler J, König M, von Deschwanden A, Hagen JO, Kääb A, Moholdt G, Pettersson R. 2013. Decadal changes from a multi-temporal glacier inventory of Svalbard. The Cryosphere 7:1603–1621. doi:10.5194/tc-7-1603-2013.

Nuttall AM, Hagen JO, Dowdeswell J. 1997. Quiescent-phase changes in velocity and geometry of Finsterwalderbreen, a surge-type glacier in Svalbard. Annals of Glaciology 24:249–254. doi:10.3189/S0260305500012258.

Östling M, Hooke RL. 1986. Water Storage in Storglaciären, Kebnekaise, Sweden. Geografiska Annaler: Series A, Physical Geography 68:279–290. doi:10.1080/04353676.1986.11880180.

Ottesen D, Dowdeswell J, Bellec V, Bjarnadóttir L. 2017. The geomorphic imprint of glacier surges into open-marine waters: Examples from eastern Svalbard. Marine Geology 392:1–29. doi:10.1016/j.margeo.2017.08.007.

Ottesen D, Dowdeswell JA. 2006. Assemblages of submarine landforms produced by tidewater glaciers in Svalbard. Journal of Geophysical Research 111. doi:10.1029/2005JF000330.

Paul F. 2015. Revealing glacier flow and surge dynamics from animated satellite image sequences: examples from the Karakoram. The Cryosphere 9:2201–2214. doi:10.5194/tc-9-2201-2015.

Reusche M, Winsor K, Carlson AE, Marcott SA, Rood DH, Novak A, Roof S, Retelle M, Werner A, Caffee M, Clark PU. 2014. ^{10}Be surface exposure ages on the late-Pleistocene and Holocene history of Linnébreen on Svalbard. Quaternary Science Reviews 89:5–12. doi:10.1016/j.quascirev.2014.01.017.

RGI. 2017. Randolph Glacier Inventory 6.0. doi:10.7265/N5-RGI-60. Type: dataset.

Robin GDQ. 1975. Velocity of radio waves in ice by means of a bore-hole interferometric technique. Journal of Glaciology 15:151–159. doi:10.3189/S0022143000034341.

Schomacker A, Benediktsson ÍÖ, Ingólfsson Ó. 2014. The Eyjabakkajökull glacial landsystem, Iceland: Geomorphic impact of multiple surges. Geomorphology 218:98–107. doi:10.1016/j.geomorph.2013.07.005.

Schytt V. 1969. Some comments on glacier surges in eastern Svalbard. Canadian Journal of Earth Sciences 6:867–873. doi:10.1139/e69-088.

Sevestre H, Benn DI. 2015. Climatic and geometric controls on the global distribution of surge-type glaciers: implications for a unifying model of surging. Journal of Glaciology 61:646–662. doi:10.3189/2015JoG14J136.

Sevestre H, Benn DI, Hulton NRJ, Baelum K. 2015. Thermal structure of Svalbard glaciers and implications for thermal switch models of glacier surging. Journal of Geophysical Research: Earth Surface 120:2220–2236. doi:10.1002/2015JF003517.

Sevestre H, Benn DI, Luckman A, Nuth C, Kohler J, Lindbäck K, Pettersson R. 2018. Tidewater Glacier Surges Initiated at the Terminus. Journal of Geophysical Research: Earth Surface 123:1035–1051. doi:10.1029/2017JF004358.

Sharp M. 1985. "Crevasse-Fill" Ridges—A Landform Type Characteristic of Surging Glaciers? Geografiska Annaler: Series A, Physical Geography 67:213–220. doi:10.1080/04353676.1985.11880147.

Sletten K, Lysså A, Lønne I. 2008. Formation and disintegration of a high-arctic ice-cored moraine complex, Scott Turnerbreen, Svalbard. Boreas 30:272–284. doi:10.1111/j.1502-3885.2001.tb01046.x.

Steel RJ, Dalland A, Larsen V. 1981. The Central Tertiary Basin of Spitsbergen: Sedimentary Development of a Sheared-Margin Basin. Geology of the North Atlantic Borderlands 7:647–664.

Stenborg T. 1970. Delay of Run-Off from a Glacier Basin. Geografiska Annaler. Series A, Physical Geography 52:1–30. Publisher: [Wiley, Swedish Society for Anthropology and Geography].

Svendsen JI, Mangerud J. 1997. Holocene glacial and climatic variations on Spitsbergen, Svalbard. The Holocene 7:45–57. doi:10.1177/095968369700700105.

Sverdrup HU, Ahlmann HW. 1935. Scientific Results of the Norwegian-Swedish Spitsbergen Expedition in 1934. Part I-III. Geografiska Annaler 17:22. doi: 10.2307/519951.

van Pelt W, Pohjola V, Pettersson R, Marchenko S, Kohler J, Luks B, Hagen JO, Schuler TV, Dunse T, Noël B, Reijmer C. 2019. A long-term dataset of climatic mass balance, snow conditions and runoff in Svalbard (1957–2018). The Cryosphere Discussions :1–30doi:10.5194/tc-2019-53.

van Pelt WJJ, Pohjola VA, Reijmer CH. 2016. The Changing Impact of Snow Conditions and Refreezing on the Mass Balance of an Idealized Svalbard Glacier. Frontiers in Earth Science 4. doi:10.3389/feart.2016.00102.

Werner A. 1993. Holocene moraine chronology, Spitsbergen, Svalbard: lichenometric evidence for multiple Neoglacial advances in the Arctic. The Holocene 3:128–137. doi:10.1177/095968369300300204.

Westergaard KB, Alsos IG, Popp M, Engelskjøn T, Flatberg KI, Brochmann C. 2011. Glacial survival may matter after all: nunatak signatures in the rare European populations of two west-arctic species: GLACIAL SURVIVAL MAY MATTER AFTER ALL. Molecular Ecology 20:376–393. doi:10.1111/j.1365-294X.2010.04928.x.

Willis MJ, Zheng W, Durkin WJ, Pritchard ME, Ramage JM, Dowdeswell JA, Benham TJ, Bassford RP, Stearns LA, Glazovsky AF, Macheret YY, Porter CC. 2018. Massive destabilization of an Arctic ice cap. Earth and Planetary Science Letters 502:146–155. doi:10.1016/j.epsl.2018.08.049.

Wilson NJ, Flowers GE. 2013. Environmental controls on the thermal structure of alpine glaciers. The Cryosphere 7:167–182. doi:10.5194/tc-7-167-2013.